

544840



Sandia National Laboratories
Operated for the U.S. Department of Energy by
Sandia Corporation

Carlsbad, New Mexico 88220

Date: November 17, 2006

To: Eric D. Vugrin, MS 1395 (Org. 6821)

Laurence H. Brush G. T. Roselle

From: Laurence H. Brush and Gregory T. Roselle, MS 1395 (Org. 6712)

Subject: Geochemical Information for Calculation of the MgO Effective Excess Factor

1 INTRODUCTION

This memorandum provides geochemical information required to calculate the effective excess factor for the magnesium oxide (MgO) being emplaced in the U.S. Department of Energy's (DOE's) Waste Isolation Pilot Plant (WIPP).

The DOE is emplacing MgO in the WIPP to serve as the engineered barrier by decreasing the solubilities of the actinide elements in transuranic (TRU) waste, such as uranium, thorium, neptunium, and plutonium. MgO will decrease actinide solubilities by consuming carbon dioxide (CO₂) that could be produced by microbial consumption of cellulosic, plastic, and rubber (CPR) materials in the TRU waste or waste containers in the repository and by controlling the pH of any brine present.

The MgO excess factor has been defined as the ratio of the total amount of MgO to be emplaced in the WIPP divided by the total amount required to consume all CO₂ that would be produced by microbial consumption of all CPR materials in the repository, calculated as specified by the U.S. Environmental Protection Agency (EPA) (Marcinowski, 2004).

This and other information needed to calculate the MgO effective excess factor were requested by the EPA as part of its review of a request by the DOE (Moody, 2006) to reduce the amount of excess MgO that it is required to emplace in the WIPP (Marcinowski, 2004). After the DOE submitted its request, the EPA asked that all uncertainties related to the MgO excess factor be described and that their effects be included to the extent possible. The MgO effective excess factor differs from the excess factor in that the former includes all uncertainties that can be quantified.

This memorandum provides information on the following aspects of the geochemical behavior of MgO in the WIPP that could affect the effective excess factor: (1) the concentrations of the main reactive phases in MgO from two of the three vendors that have supplied this material to the DOE

Exceptional Service in the National Interest

SNL/WIPP Records Center File Code: WIPP:1.4.1.2:PA:QA-L:543621-11/21/06

543261
RH

1 of 36

(Section 2), (2) our expectation as to how much of these phases will actually react with CO₂ (Section 3), (3) the number of moles of CO₂ that will be consumed per mole of MgO emplaced in the repository (Section 4), (4) natural analogs and experimental studies that show that periclase hydrates to form brucite if H₂O is present, that brucite carbonates to form magnesite or hydromagnesite if CO₂ is present, and that hydromagnesite will dehydrate to form magnesite in less than 10,000 years (Section 5); (5) the likelihood of and extent to which CO₂ will be consumed by other materials (Section 6). This memorandum replaces and expands on the memorandum provided in a draft dated June 21, 2006, for transmittal to the EPA.

In this memorandum, "MgO" refers to the bulk, granular material being emplaced in the WIPP to serve as the engineered barrier. MgO comprises mostly periclase (pure, crystalline MgO – the main reactive constituent of the engineered barrier), which will consume CO₂ and water (H₂O) and form brucite (Mg(OH)₂), hydromagnesite (Mg₅(CO₃)₄(OH)₂·4H₂O), and – eventually - magnesite (MgCO₃). The terms "periclase," "brucite," "hydromagnesite," and "magnesite" are mineral names and should, therefore, be restricted to naturally occurring forms of materials that meet all other requirements of the definition of a mineral (see, for example, Bates and Jackson 1984). However, mineral names are used herein for convenience.

MgO will decrease actinide solubilities by consuming essentially all CO₂ that would be produced by microbial consumption of all CPR materials in TRU waste or waste containers in the repository. Although MgO will consume nearly all CO₂, small quantities (relative to the quantity that would be produced by microbial consumption of all CPR materials) will persist in the aqueous and gaseous phases. The residual quantity will be so small relative to the initial quantity that the adverb "essentially" is omitted hereafter in this memorandum. Subsection 6.4 (see below) demonstrates how small the residual quantity of CO₂ will be for the case of the CO₂ dissolved in WIPP brines.

2 CONCENTRATIONS OF REACTIVE CONSTITUENTS IN MgO

This section provides the concentrations of the reactive constituents of the MgO supplied by Premier Chemicals and Martin Marietta Magnesia Specialties. We are unaware of any information on the concentrations of the reactive constituents of the MgO provided by National Magnesia Chemicals. However, National Magnesia MgO was emplaced in only one disposal room in the WIPP (see below).

Periclase is the main reactive constituent of Premier and Martin Marietta MgO. Lime (CaO), another reactive constituent that is present in Premier MgO and appears to be present in Martin Marietta MgO, will also consume CO₂ and H₂O and form portlandite (Ca(OH)₂) and calcite. However, if present, lime: (1) is much less abundant than periclase (see Subsections 2.1 and 2.2 below), (2) will consume much less CO₂ and H₂O than will periclase, and (3) will have relatively little effect on near-field chemical conditions (i.e., pH).

2.1 Vendors That Have Provided MgO to the WIPP

The three vendors that have provided MgO since the WIPP opened on March 26, 1999 are: (1) National Magnesia Chemicals, which supplied the MgO emplaced in the WIPP from late March 1999 (Panel 1, Room 7) through mid-April 2000 (Panel 1, Room 7); (2) Premier Chemicals,

which provided the MgO emplaced from mid-April 2000 (Panel 1, Room 7) through late December 2004 or early January 2005 (Panel 2, Room 2); and (3) Martin Marietta Magnesia Specialties LLC, which supplied the material emplaced since late December 2004 or early January 2005 (Panel 2, Room 2). Note that, in every seven-room WIPP panel, waste is emplaced in Room 7 first and in Room 1 last. We thank Steve Casey of the U.S. DOE's Carlsbad Field Office for providing this information.

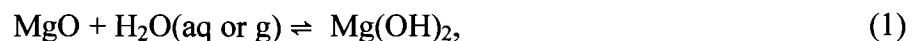
2.2 Premier MgO

Premier MgO contains about 90 wt % periclase and lime and ~10 wt % nonreactive phases (U.S. DOE, 2004, Appendix BARRIERS, p. 5). The nonreactive phases include oxides and silicates such as spinel (MgAl_2O_4), ulvöspinel ($\text{Ti(Fe,Mg)}_2\text{O}_4$), forsterite (Mg_2SiO_4), and monticellite (CaMgSiO_4). These results are based on characterization of Premier MgO by Bryan and Snider (2001a) and Snider (2003a).

Bryan and Snider (2001a) reported that a typical chemical analysis of Premier MgO yields about 91 wt % MgO, 1 wt % alumina (Al_2O_3), 3 wt % silica (SiO_2), 4 wt % calcium oxide (CaO), and 1 wt % iron(III) (Fe(III)) oxide (Fe_2O_3). Most of the MgO and some of the CaO occur as periclase and lime, respectively, in Premier MgO. However, some of the MgO and CaO, and most – if not all – Al_2O_3 , SiO_2 , and Fe(III) oxide are present in the accessory oxide and silicate minerals described above.

Snider (2003a) used inductively coupled plasma-optical emission spectroscopy (ICP-OES) and gravimetric analysis to quantify the mineralogical composition of one of the lots of Premier MgO used for the experiments described below. Based on the assumption that the silicate in this MgO is forsterite, Snider (2003a) reported that this lot of MgO contains 86.86 wt % periclase, 2.386 wt % lime, 2.071 wt % spinel, and 5.02 wt % forsterite. If the silicate is monticellite, this lot contains 88.73 wt % periclase, 1.273 wt % lime, 2.071 wt % spinel, and 5.756 wt % monticellite. Given the uncertainties inherent in quantifying the mineralogical composition of materials such as Premier MgO, it is reasonable to conclude that this material contains ~90 wt % periclase and lime and ~10 wt % of nonreactive oxides and silicates.

It was reported (U.S. DOE, 2004, Appendix BARRIERS, p. 8) that hydration of Premier MgO, which proceeds via the reaction



reached completion after formation of about 85 mol % brucite. This conclusion was based on the observation by Snider (2002, Figures 1, 2, 6, and 7) that hydration of Premier MgO in accelerated experiments reached completion after formation of ~85 mol % brucite. These experiments consisted of hydration of MgO in deionized (DI) water at 90 °C, or hydration in air at 80 °C and a relative humidity (RH) of 95%. Snider (2003c) calculated that the average brucite content is 84.6 mol % after complete hydration, based on the last 8 data points of the inundated hydration experiment with DI H_2O at 90 °C (Snider 2002, Figures 1 and 2) and the last 16 data points of the humid hydration run at 80 °C and 95 % RH (Snider 2002, Figures 6 and 7). Two assumptions were made regarding these results: (1) the brucite content of the run products of an accelerated hydration experiment plus that of any unreacted periclase are equal to the periclase content of the starting materials, and (2) the periclase that reacts with aqueous or gaseous H_2O in an accelerated hydration test will also react with aqueous or

gaseous CO₂ in the WIPP. It was not assumed that hydration necessarily precedes carbonation in laboratory experiments, or that it will precede carbonation in the repository.

The conclusion that hydration of Premier MgO reached completion after formation of ~85 mol % brucite in the Snider's (2002) accelerated experiments does not agree with the result that this material contains ~90 wt % reactive phases and ~10 wt % nonreactive phases. This contradiction was resolved soon after the DOE submitted its first WIPP Compliance Recertification Application (CRA-2004) to the EPA on March 26, 2004. After submission of the CRA-2004, Snider and Xiong (2004) determined that the extent of "complete" hydration calculated by Snider (2003c) (~85 mol % brucite) and included in the CRA-2004 (U.S. DOE, 2004, Appendix BARRIERS, p. 8) was incorrect, and that the actual extent of complete hydration observed for Premier MgO in accelerated tests is ~89 mol % brucite. The reason for Snider's (2003c) mistake is that she (and other Sandia personnel) carried out the technique referred to as "loss on ignition" (LOI), used to measure the brucite content of MgO hydration products, at 500 °C – a temperature too low to dehydrate all brucite to periclase in a reasonable time. LOI at 750 °C appears to dehydrate most or essentially all brucite, although it also results in decrepitation in the case of some of the materials tested (see Subsection 2.3 below).

It is worth noting that, in addition to lime, one or more of the oxide or silicate impurities in Premier MgO might also consume significant quantities of CO₂ and H₂O in the WIPP, albeit at lower rates than periclase and lime. This is especially possible for forsterite and monticellite.

2.3 Martin Marietta Magnesia Specialties MgO

The results of Wall (2005) and Deng et al. (2006a) imply that MgO from Martin Marietta contains 96 mol % periclase and lime.

Wall (2005) carried out accelerated hydration experiments (hydration of MgO in DI water at 90 °C) to: (1) measure the concentrations of periclase and lime in these materials and to compare them to those of Premier MgO; (2) measure the accelerated hydration rates of the Martin Marietta products and to compare them to those of Premier MgO; (3) improve, if possible, the LOI technique used to measure the brucite and portlandite contents of MgO hydration products. She evaluated three materials from Martin Marietta: MagChem 10 WTS-20, MagChem 10 WTS-30, and MagChem 10 WTS-60. ("MagChem 10" is omitted hereafter.) All these products are hard-burned MgO (calcined at 1000-1500 °C) with a specified MgO content of 95 wt % and a bulk density of 87 lb/ft³. Assay results are typically 97 wt % MgO. However, these results could include MgO in phases other than periclase, such as other oxides or silicates (see Subsection 2.2 above).

Washington TRU Solutions LLC (WTS) considered her results, among other factors beyond the scope of this memorandum, during its selection of a new supplier of MgO and a specific product from that supplier. This was necessary because Premier Chemicals indicated that it could no longer provide MgO that meets the WTS specifications for the WIPP engineered barrier (WTS, 2005). WTS selected Martin Marietta's WTS-60.

Table 1 compares Wall's (2005) results for WTS-20, WTS-30, and WTS-60 with those obtained by Snider and Xiong (2004) for Premier MgO. Table 1 illustrates the effects of the materials used for the accelerated hydration experiments and the temperature used for LOI on the brucite and portlandite contents of the hydration products and – by assumption – the periclase and lime contents of these materials. Two important conclusions can be drawn from these results: (1) all three materials

from Martin Marietta have higher contents of reactive constituents than Premier MgO; (2) LOI at 750 °C yields higher brucite and portlandite contents (and, by assumption, higher initial periclase and lime contents) than LOI at 500 °C. The discussion of the results for Premier MgO (Subsection 2.2) implies that the 750 °C results are more accurate than the 500 °C results.

LOI at 750 °C was unsuccessful for WTS-20 and WTS-60 due to decrepitation of these samples at this temperature. Wall (2005) was unable to develop a procedure for LOI at 750 °C that prevented decrepitation of these samples. However, the fact that LOI for WTS-60 at 500 °C yielded a higher brucite and portlandite content than LOI with WTS-30 at this temperature strongly suggested that the sample of WTS-60 tested by Wall (2005) had a periclase and lime content greater than or equal to that of WTS-30, and that the brucite and portlandite content of WTS-60 from LOI at 750 °C would equal or exceed 96 mol %, or 97 wt % (see Table 1). Therefore, it seemed reasonable to conclude that WTS-60, the MgO that is currently being emplaced in the WIPP, contains 96 mol % (97 wt %) periclase and lime.

Another important result of Wall's (2005) work is that Martin Marietta MgO hydrated significantly faster in accelerated hydration experiments than Premier MgO at the same temperature (90 °C). Although we do not have any 25 °C hydration data for Martin Marietta MgO yet, comparison of the 90 °C data suggests that Martin Marietta MgO will hydrate faster - and carbonate faster - than Premier MgO at 28 °C, the temperature in the undisturbed Salado Fm. at the repository horizon and hence the temperature expected in the repository after it is filled and sealed (Munson et al., 1987).

Deng et al. (2006a) are carrying out a laboratory study of the efficacy of Martin Marietta MgO. For that study, Deng et al. (2006b) conducted chemical, and LOI and thermal gravimetric (TGA) analyses of WTS-60. They analyzed for Mg, Ca, Al, Fe, and Si by gravimetric determination of SiO₂, which involved: (1) dissolution in nitric acid, (2) analysis of the liquid by ICP-AES, and (3) weighing the remaining solids (Deng et al, 2006b, Appendix B, Subsection B.1). They performed LOI and TGA by determining the weight percent of H₂O released by hydrated MgO from 150-800 °C and assuming that nonreactive components do not hydrate to a significant extent and that any unbound water will be lost at temperatures below 150 °C (Deng et al., 2006b, Appendix B, Subsection B.2). Table 2 provides the combined results of these analyses.

Results from Deng et al. (2006) suggest that the impurities in WTS-60 are: (1) a spinel-group mineral that appears to be a solid solution of the four end members chromite (FeCr₂O₄), hercynite (FeAl₂O₄), magnesiochromite (MgCr₂O₄), and spinel (MgAl₂O₄); (2) hematite (Fe₂O₃); and (3) SiO₂ (polymorph yet to be determined). The relative proportions of these phases are also yet to be determined. It is possible that one or more of these impurities could also consume significant quantities of CO₂ and H₂O in the WIPP, albeit at lower rates than periclase and lime.

2.3.1 Variability of the Composition of Martin Marietta MgO

All MgO provided by Martin Marietta must meet the requirements specified by WTS (2005). Regarding its chemical composition, WTS (2005, p. 2, Subsection 3.3.1, Item A) specifies that:

“The sum of magnesium oxide (MgO) plus calcium oxide (CaO) shall be a minimum of 95%, with MgO being no less than 90%. The remainder of the material shall not contain any items considered hazardous to people or the environment.”

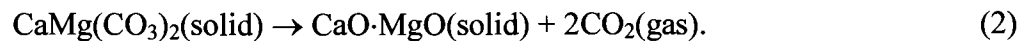
Information Only

WTS (2005) does not specify the mineralogical composition of the MgO used for the WIPP engineered barrier. However, it does specify that it pass a reactivity test (WTS, 2005, Attachment B). This test requires that the average maximum temperature increase observed in triplicate runs carried out by placing 18 g of the MgO in a 400 mL glass beaker containing 300 g of 20% phosphoric acid be at least 20 °C. Clearly, all MgO emplaced in the WIPP will meet these requirements, as well as all other requirements specified by WTS (2005).

The process used by Martin Marietta to manufacture its “hard-burned” MgO is summarized below. This summary is based on information obtained from the Martin Marietta website (Martin Marietta Magnesia Specialties, 2006).

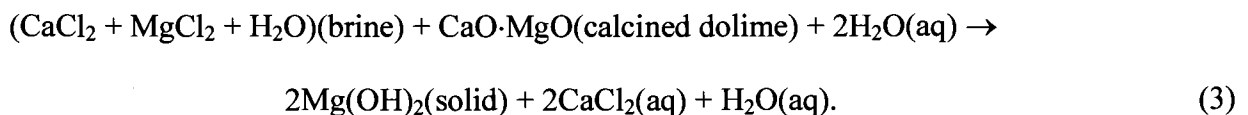
Martin Marietta pumps brine from a depth of about 2,500 ft in the Michigan Basin. According to the information on their website, this brine consists of $\text{CaCl}_2 + \text{MgCl}_2 + \text{H}_2\text{O}$. This formula does not include solutes such as Na^+ , K^+ , and SO_4^{2-} , which are important constituents of WIPP brines and presumably are present in brines from the Michigan Basin.

Martin Marietta obtains calcined dolime by calcining dolomitic limestone (represented by $\text{CaMg}(\text{CO}_3)_2(\text{solid})$ below and hereafter referred to as “dolomite”) quarried in Ohio. The reaction is:



Again, the formula for dolomite does not include impurities such as clay minerals and quartz (SiO_2), which presumably are present in small quantities in the dolomite used for this process.

They then mix the brine with calcined dolime and water to produce a slurry containing dissolved CaCl_2 and particulate $\text{Mg}(\text{OH})_2$ via the reaction:



Note that H_2O was included on both sides of Reaction 3 to be consistent with the information on the Martin Marietta website.

Next, the brucite is allowed to settle. It is filtered and washed to remove all brine and the CaCl_2 dissolved in this brine.

Finally, it is hard-burned (calcined at 1000-1500 °C) to convert brucite to periclase via the reaction:



Hard burning results in a product that is more reactive than “dead-burned” MgO (calcined at 1500-2000 °C), but less reactive than “light-burned” MgO (calcined at 700-1000 °C).

WTS chose Martin Marietta as the supplier of MgO for the WIPP after Premier Chemicals informed WTS that it was running out of ore that was high enough in grade to produce MgO that contained a minimum of 95% MgO + CaO, with MgO being no less than 90%. WTS replaced Premier

with Martin Marietta before Premier ran out of suitable ore, and all MgO supplied by Premier continued to meet the compositional (and other) requirements specified by WTS (2005). Therefore, it is reasonable to assume that all MgO emplaced in the WIPP in the future will continue to meet these requirements, subject to any revisions in the WTS specifications.

Beyond that, however, it is difficult to predict whether the chemical composition of the brine, or the chemical and mineralogical compositions of the dolomite will vary enough to affect the results shown in Table 1 (see above). In particular, we do not know the grades, tonnages, or grade-tonnage relationships of Martin Marietta's proven reserves of brine and dolomite; or the ease with which alternative sources could be developed if the proven reserves were insufficient to meet the long-term requirements of the WIPP Project. It is also unclear if the compositional variations in the brine and dolomite are greater or less than those associated with a sedimentary magnesite deposit such as the one at Gabbs, NV, that Premier used to produce MgO.

2.4 Implications for the MgO Effective Excess Factor

Incorporation of the effect of the concentration of reactive constituents in Premier MgO into the MgO effective excess factor necessitates multiplication of the other terms in the effective excess factor by 0.89, because LOI analysis of Premier MgO hydrated in accelerated tests yielded 89 mole % periclase and lime (see Table 1). However, Premier MgO was emplaced only in Panel 1, Room 7; through Panel 2, Room 2, or about six-seven rooms.

Inclusion of the concentration of reactive constituents in Martin Marietta MgO requires multiplication of the effective excess factor by 0.96, because analysis by Deng et al. (2006a) yielded 96 mole % periclase and lime (Table 2). Martin Marietta MgO has been emplaced since Panel 2, Room 2.

3 EXPECTED EXTENT OF REACTION OF PERICLASE AND/OR BRUCITE WITH CO₂

All results to date from studies carried out for the WIPP Project imply that the periclase and lime present in MgO will be available to react – and will continue to react - until all CO₂ in the repository has been consumed.

3.1 Experiments with Reagent-Grade and WIPP MgO

Experiments were carried out during the mid-to-late 1990s at Sandia National Laboratories (SNL) in Albuquerque, after MgO was added to the WIPP disposal system in 1996 (see, for example, SNL, 1997; Zhang et al., 2000). These experiments were conducted for the most part with reagent-grade materials under accelerated conditions. MgO was also added to one of the containers in the WIPP Source Term Test Program (STTP) at Los Alamos National Laboratory. The STTP was a series of tests with actual TRU waste (see, for example, Villarreal et al., 2001a; 2001b; 2001c; 2001d). The STTP comprised 39 liter-scale and 15 drum-scale experiments.

The New Mexico Environmental Evaluation Group cited one STTP test (L-28) in which MgO was apparently ineffective (Oversby, 2000). L-28, one of 39 liter-scale tests, was carried out at

a CO₂ pressure of 60 bars, several orders of magnitude higher than that expected in the WIPP (~10^{-5.5} atm). The partial pressure of CO₂ in the WIPP will not exceed ~10^{-5.5} atm because the rate of CO₂ consumption by the periclase and/or brucite and lime and/or portlandite in MgO is much higher than the microbial CO₂ production rate. Therefore, the conditions in L-28 were not representative of those expected in the WIPP, and the results are irrelevant to the WIPP.

Nevertheless, Bryan and Snider (2001b, p. 5-9) and Snider (2002, pp. 3.1-13-3.1-15) conducted a series of “cemented-cake” experiments to determine whether lithification of MgO will occur in the WIPP and, if so, whether it would affect the rate of hydration of MgO. For their experiments, started in June 2001, they placed 15, 30, or 45 g of Premier MgO in 125-mL plastic containers with Energy Research and Development Administration (WIPP Well) 6 (ERDA-6) or Generic Weep Brine (GWB). ERDA-6 is a synthetic brine representative of fluids in brine reservoirs in the Castile Formation (Fm.) (Popielak, et al., 1983). GWB is a synthetic brine typical of intergranular (grain-boundary) fluids from the Salado Fm. at or near the stratigraphic horizon of the repository (Snider, 2003b). This resulted in a 5-, 10-, or 15-mm thick layer of Premier MgO at the bottom of the containers. They then placed the containers in ovens at 25, 50, 70, or 90 °C. They did not agitate them. (Agitation apparently prevented any lithification of MgO in their other inundated experiments.)

Snider (2002, Figures 12-14) reported results from cemented-cake experiments that lasted for periods of about four to six months. She observed lithification of some of the samples; however, others remained “very friable,” even after inundation at 70 and 90 °C (Snider, 2002, p. 3.1-15). Snider (2002, p. 3.1-13) had “anticipated that the thicker layers would hydrate at a slower rate,” especially if lithification occurred. However, she reported that, “MgO thickness has not affected the hydration rate under inundated conditions in ERDA-6 (Figure 12)” (Snider, 2002, p. 3.1-13); and that, “in GWB at 50, 70, and 90° C (Figure 13) thickness does not affect hydration” (Snider, 2002, p. 3.1-15). Furthermore, the 5-mm-thick samples in GWB at 25 °C hydrated at the slowest rate; the 15-mm-thick samples hydrated at an intermediate rate; and the 10-mm-thick samples hydrated at the fastest rate (Snider, 2002, Figure 13). Therefore, these experiments did not show that lithification will occur, or that - if it does - it will decrease the MgO hydration rate.

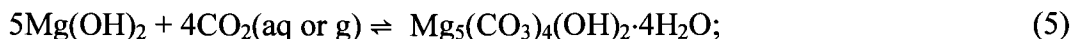
Clearly, proving that a process will not occur in 10,000 years is very difficult. However, it can be said that all results to date - either from studies carried out for the WIPP Project or those for other applications - imply that the periclase present in MgO will continue to react until all CO₂ is consumed. Therefore, periclase and lime in MgO will remain available to react – and will continue to react – until all CO₂ in the repository has been consumed.

3.2 Implications for the MgO Effective Excess Factor

Because all results to date imply that the periclase and lime present in MgO will be available to react – and will continue to react - until all CO₂ in the repository has been consumed, the MgO effective excess factor need not be reduced to account for incomplete reaction. This is consistent with multiplication of the excess factor by 1.

4 THE NUMBER OF MOLES OF CO₂ CONSUMED PER MOLE OF PERICLASE

The number of moles of CO₂ that will be consumed per mole of periclase in the MgO emplaced in the WIPP will depend on whether the MgO carbonation product is hydromagnesite or magnesite. The brucite carbonation reactions that produce hydromagnesite and magnesite are:



According to these equations, formation of hydromagnesite would consume 0.8 mole of CO₂ per mol of periclase; formation of magnesite would consume 1 mole of CO₂ per mole of periclase. (The concentrations of periclase in the Premier and Martin Marietta MgO emplaced in the repository are discussed above in Subsections 2.1 and 2.2, respectively.) Similar reactions could be written for the hydration and carbonation of periclase, but the number of moles of CO₂ consumed per mole of MgO would be the same.

Subsequent conversion of hydromagnesite to magnesite would consume additional CO₂ and release H₂O:



Therefore, the reaction of brucite to form hydromagnesite followed by the conversion of hydromagnesite to magnesite (Reaction 5 followed by Reaction 7) would result in the overall consumption of 1 mole of CO₂ per mole of periclase, the same ratio as that obtained by the formation of magnesite directly from brucite (Reaction 6).

Hydromagnesite will be the dominant Mg carbonate for the early part of the 10,000-year regulatory period. However, magnesite will replace hydromagnesite rapidly enough to be the dominant Mg carbonate for most of the 10,000-year regulatory period.

4.1 Experimental and Modeling Studies of Mg Carbonation, and Field Observations of Mg Carbonates in The Delaware Basin

The DOE maintained in the WIPP Compliance Certification Application (CCA) that magnesite will be the Mg carbonate present throughout the 10,000-year regulatory period (U.S. DOE, 1996, Appendix BACK; U.S. DOE, 1996, Appendix SOTERM). This conclusion was based on calculations by Novak et al. (1996) with the geochemical speciation component of the Fracture-Matrix Transport (FMT) code (Babb and Novak, 1995), which demonstrated that magnesite is thermodynamically stable with respect to hydromagnesite and other Mg carbonates under expected WIPP conditions. Because magnesite is the stable Mg carbonate, the DOE maintained that the brucite-magnesite carbonation reaction (see Reaction 6 above) would buffer f_{CO_2} in the repository at a value of $10^{-6.9}$ atm, and used

this value of f_{CO_2} (along with other parameters) to calculate actinide speciation and solubilities for the CCA performance assessment (PA).

Recent thermodynamic calculations carried out by Brush and Xiong (2003a, 2003b, 2005) and Brush (2005) with the EQ3/6 geochemical software package (Daveler and Wolery, 1992; Wolery, 1992a; 1992b; Wolery and Daveler, 1992) and FMT (Babb and Novak, 1997 and addenda; Wang, 1998) also imply that magnesite is stable with respect to both hydromagnesite and other Mg carbonates under expected WIPP conditions.

Furthermore, magnesite is commonly observed in the Salado Fm. (Lang, 1939; Adams, 1944; Lowenstein, 1983; 1988; Stein, 1985) and in other formations in the Delaware Basin (Garber et al., 1990). Lowenstein (1988, p. 598) describes the siliciclastic-carbonate mudstone in which magnesite is most abundant in the Salado as a "non-evaporitic sediment" and attributes its origin to subaqueous "settling of fine-grained, suspended material in the center of the Salado basin where the energy of inflow waters had largely dissipated." Therefore, the magnesite observed in the Salado did not necessarily form in situ. However, Garber et al. (1990), who reported that magnesite "occurs pervasively" throughout an 82-m (270-ft) interval of core recovered from a stratigraphic test well located along the subsurface trend of the Capitan Reef 27 km (17 miles) northeast of Carlsbad, concluded that "the most likely origin for the magnesite in the core is the downward movement of dense fluids from the Ochoan Series, Salado Formation into the underlying, and [at the time] shallowly buried Tansil and Yates formations." Clearly, magnesite either formed or persisted for long periods in the Delaware Basin. Therefore, the possibility that significant quantities of magnesite could form from carbonation of MgO during the 10,000-year regulatory period cannot be ruled out.

During its review of the CCA, the EPA questioned the DOE's conclusion that magnesite will be present throughout the entire 10,000-year regulatory period. For the CCA, the DOE based this conclusion on the fact that magnesite is the thermodynamically stable Mg carbonate under expected WIPP conditions (U.S. DOE, 1996, Appendix BARRIERS and Appendix SOTERM). The EPA accepted the DOE's assertion that magnesite is stable, but questioned whether the kinetics of the hydromagnesite-magnesite reaction are fast enough to produce enough magnesite in 10,000 years for the brucite-magnesite reaction to buffer f_{CO_2} at $10^{-6.9}$ atm. Therefore, SNL (1997) presented additional evidence that magnesite would form in 10,000 years. In particular, SNL (1997) used an Arrhenius extrapolation of the effects of temperatures from 60 to 180 °C on the rates of magnesite formation from two separate experimental studies carried out for applications other than the WIPP Project to conclude that magnesite formation would occur in a few hundred years at 28 °C, the temperature expected in the repository after it is filled and sealed (Munson et al., 1987).

Based on this evidence, the EPA (U.S. EPA, 1998) concluded that:

"The available rate data indicate that some portion, perhaps all, of the hydromagnesite will be converted to magnesite over the 10,000-year period for repository performance. The exact time required for complete conversion has not been established for all chemical conditions. However, the available laboratory and field data clearly indicate that magnesite formation takes from few hundred to, perhaps, a few thousand years. Thus, the early repository conditions can be best represented by the equilibrium between brucite and hydromagnesite. These conditions will eventually evolve to equilibrium between brucite and magnesite."

However, the EPA also stated in the same document that:

“These estimates of conversion rate are confounded by the fact that deposits of hydromagnesite are found in some evaporite basins dated as late Quaternary in age (<23.7 million years) (Stamatakis, 1995), indicating that the hydromagnesite has persisted in a metastable state for a long period with only partial conversion to magnesite and other magnesium carbonates.”

Based at least in part on its interpretation of the implications of the huntite- $(\text{CaMg}_3(\text{CO}_3)_4)$ -hydromagnesite deposits described by Stamatakis (1995) for the kinetics of the hydromagnesite-magnesite reaction, the EPA stipulated that the brucite-hydromagnesite (5424) reaction be used to buffer f_{CO_2} for the actinide-solubility calculations for its 1997 Performance Assessment Verification Test (PAVT) (Trovato, 1997; U.S. EPA, 1998). This reaction buffers f_{CO_2} at a value of $10^{-5.5}$ atm, a value somewhat higher than the value of $10^{-6.9}$ atm maintained by the brucite-magnesite reaction, which was used for the CCA PA. We have used a value of $10^{-5.5}$ atm for f_{CO_2} for WIPP PA since the PAVT. However, we reconsider the implications of Stamatakis (1995) for the kinetics of the hydromagnesite-magnesite reaction and the number of moles of CO_2 consumed per mole of periclase in Subsection 5.3 (see below).

Most of the experimental work carried out for the WIPP Project since the CCA has yielded hydromagnesite as the carbonation product of brucite (or periclase). Bryan and Snider (2001a, 2001b), Snider (2002), Snider and Xiong (2002), and Xiong and Snider (2003) carried out carbonation experiments with Premier MgO and reagent-grade periclase under humid and inundated conditions. Inundated experiments were carried out with 5 g of uncrushed Premier MgO in 100 mL of DI H_2O , 4.00-M NaCl, ERDA-6, or GWB under an atmosphere consisting of compressed, ambient, laboratory air at room temperature for up to 327 days. Inundated experiments were also conducted with uncrushed Premier MgO; crushed, prehydrated Premier MgO; Fisher reagent-grade periclase; or prehydrated Fisher periclase in 100 mL of ERDA-6 or GWB under an atmosphere containing 5% CO_2 at room temperature for periods up to 91 days (Snider and Xiong, 2002). Humid experiments were performed at room temperature and 40 °C in compressed, ambient, laboratory air at an RH of 33, 58, 75, or 95%.

Snider and Xiong (2002) detected hydromagnesite with the composition $\text{Mg}_5(\text{CO}_3)_4(\text{OH})_2 \cdot 4\text{H}_2\text{O}$ with X-ray diffraction (XRD) analysis of the solids from inundated experiments with ERDA-6 and atmospheric CO_2 . No other Mg carbonates were detected in runs with ERDA-6 and atmospheric CO_2 . Snider and Xiong (2002) detected both hydromagnesite and nesquehonite ($\text{MgCO}_3 \cdot 3\text{H}_2\text{O}$) with XRD analysis of solids from experiments with ERDA-6 and an atmosphere containing 5% CO_2 , but hydromagnesite was clearly replacing nesquehonite as these runs proceeded. In experiments with GWB, hydromagnesite was the only Mg carbonate detected by Snider and Xiong (2002). Hydromagnesite was also the only Mg carbonate observed in their humid experiments. Formation of magnesite was never observed in any of these experiments. Therefore, these experiments suggest that hydromagnesite will be the dominant Mg carbonate early in the 10,000-year WIPP regulatory period.

However, experiments carried out for the WIPP Project in the late 1990s by Zhang et al (2000) imply that magnesite will replace hydromagnesite rapidly enough to be the dominant Mg carbonate for most of the 10,000-year regulatory period. Zhang et al. (2000) studied the conversion of hydromagnesite to magnesite in a saturated NaCl solution and GWB at high temperatures and used the Arrhenius equation to extrapolate the results to 25 °C, which is close to 28 °C (the temperature expected in the repository after it is filled and sealed; see Munson et al., 1987). Zhang et al. (2000)

reacted 0.3 g of reagent-grade hydromagnesite with 1.5 g of saturated NaCl solution or GWB in autoclaves (type unspecified) at 110, 150, or 200 °C. They then quantified the extent of conversion attained in their experiments by comparing XRD patterns for their samples with XRD calibration curves obtained by running premixed samples of their reagent-grade hydromagnesite and reagent-grade magnesite.

Zhang et al. (2000) found that, after an induction period that persisted for nearly half of the time required for essentially complete conversion of hydromagnesite to magnesite and during which only a few percent of the hydromagnesite reacted to form magnesite, conversion took place in weeks to days at 110 and 150 °C. At 200 °C, conversion took place in a few to several hours. (At room temperature, formation of magnesite has never been observed in experiments carried out for the WIPP Project, even in experiments that lasted for a few years.) Conversion of hydromagnesite to magnesite appeared to be a first-order reaction. The induction period, during which about 4-5% of the hydromagnesite formed magnesite, may have resulted from slow nucleation of magnesite, after which magnesite formed rapidly.

Zhang et al (2000) also observed that conversion was faster in saturated NaCl than in GWB. (All experiments carried out subsequently with Premier MgO have also shown that the rates of hydration and carbonation of periclase and brucite occurred faster in simpler, less concentrated solutions than in complex solutions with higher ionic strengths; i.e., the rates of reaction decrease in the order DI H₂O > 4 M NaCl > ERDA-6 > GWB.)

Based on their extrapolations to 25 °C, Zhang et al. (2000) concluded that after an induction period of 18 or 200 years in saturated NaCl or GWB, respectively, the “half life” of hydromagnesite (the time required for conversion of half of the hydromagnesite to magnesite) would be 4.7 years (saturated NaCl) or 73 years (GWB). A period of about 1000 years, the sum of the 200-years and 730 years (10 half lives), would result in conversion of over 99.9% of any hydromagnesite present to magnesite. Clearly, this would ensure that the MgO engineered barrier would consume very close to 1 mol of CO₂ per mol of periclase.

Any hydromagnesite formed prior to 9,000 years after the WIPP is filled and sealed would convert completely to magnesite, which – along with the initially formed hydromagnesite – would consume 1 mole of CO₂ per mole of periclase. Furthermore, much of the hydromagnesite formed after 9,000 years would react to form magnesite.

The uncertainties inherent in the extrapolated results of Zhang et al (2000) are probably significantly less than those in SNL (1997) because Zhang et al (2000) used high-ionic-strength brines - including one WIPP brine (GWB) - for their experiments, but SNL (1997) used only low-ionic-strength (~0.05 M) results obtained from the literature.

4.2 Implications for the MgO Effective Excess Factor

Incorporation of the ratio of the number of moles of CO₂ consumed per mole of periclase in MgO into the effective excess factor necessitates multiplication of this factor by a value close to 1. The number of moles of CO₂ consumed per mole of periclase will be close to 1 because: (1) magnesite will be the dominant Mg carbonate throughout most of the 10,000-year regulatory period; and (2) formation of magnesite from brucite (or periclase), and formation of hydromagnesite followed by conversion of hydromagnesite to magnesite would both consume 1 mol of CO₂ per mol of periclase.

The exact ratio of CO₂ consumed per mol of periclase will depend on how much CO₂ is produced by microbial activity prior to 9,000 years. Therefore, this ratio might have to be computed on a vector-by-vector basis.

5 ANALOGS AND EXPERIMENTAL STUDIES THAT SHOW THAT PERICLASE WILL HYDRATE AND THAT BRUCITE WILL CARBONATE

Results from studies carried out for the WIPP Project imply that the periclase and lime present in MgO will be available to react – and will continue to react - until all CO₂ in the repository has been consumed (see Section 4 above). Furthermore, results from other studies conducted for the WIPP Project imply that, although hydromagnesite will be the dominant Mg carbonate for the early part of the 10,000-year regulatory period, magnesite will replace hydromagnesite rapidly enough to be the dominant Mg carbonate for most of the 10,000-year regulatory period.

Nevertheless, we have carried out a literature search for anthropogenic or natural analogs, or experimental studies that confirm our conclusion that hydration of periclase to form brucite, and carbonation of brucite to form hydromagnesite will proceed to completion if H₂O or CO₂, respectively, are present (see Subsections 5.1 and 5.3 below). Furthermore, we considered a reported occurrence of hydromagnesite that has apparently persisted for a period much longer than the 10,000-year WIPP regulatory period (Subsection 5.3).

5.1 Periclase Hydration

A number of experimental studies have been conducted by the Sandia National Laboratories – Carlsbad Program Group to investigate the hydration of periclase to form brucite (Bryan and Snider, 2001a; 2001b; Snider, 2002; 2003a; Snider and Xiong, 2004; Wall, 2005). The results of these studies show that periclase used in the MgO engineered barrier will rapidly hydrate to form brucite over a time span of days to weeks. However, these experiments were conducted under “accelerated” conditions at temperatures higher than those expected in the WIPP. In response to comments from the EPA, a literature search was conducted to provide additional examples supporting the SNL-CPG experiments. These examples include lower temperature experiments and natural analogs. There are three main categories into which these studies can be grouped: (1) hydration studies using Portland cement (see Subsection 5.1.1 below), (2) natural analogs in the form of contact metamorphosed dolomites (Subsection 5.1.2), and (3) other (mainly high-temperature) experimental studies (Subsection 5.1.3).

5.1.1 Portland Cements

Crystalline periclase is a common constituent of Portland cements. It is generally seen as an undesired contaminant because of the volume increase associated with its hydration to brucite (Klemm, 2005). Excessive expansion of concrete mineral phases is of great concern because it affects the soundness of the concrete resulting in potential swelling, cracking and disintegration. Periclase is of particular concern because it hydrates more slowly than other mineral phases in the cement. As a result, the increase in volume cannot be accommodated by the still unconsolidated cement. For this reason, strict limits of 6% MgO have been imposed for Portland cements (ASTM C 150-05).

Numerous studies have been conducted to evaluate the mechanisms of periclase hydration and, ultimately, how to inhibit hydration. The effectiveness of pozzolanic additives on the hydration of periclase in cement pastes was evaluated in a long-term hydration study (Kasselouris et al., 1985). In this study a clinker that contained 8.44% free periclase was used to prepare a cement paste. A series of pastes were produced using different types and amounts of pozzolanic additives. Most importantly for the WIPP MgO analysis, however, is that these studies also used a pozzolan-free sample as a control experiment. Each of the pastes was cured in potable water at 18 ± 2 °C for periods of up to 12 years. The percentage of hydrated MgO in the experiments was determined annually using differential thermal analysis. The results show that the pure cement reached a maximum hydration percentage of 74% at 6 years. Beyond this time little to no additional hydration was observed.

A similar study by Qing et al. (2004) looked at the expansion of low heat Portland slag cement with slight expansion due to the hydration of periclase and gypsum. In this study a clinker containing 2.8 to 3.1% periclase was used to prepare a cement paste. The paste was then cured in water at 20 ± 2 °C for 2,000 days. Samples were then periodically analyzed using scanning electron microscopy and XRD analysis. The results show that periclase hydration in the paste started at approximately 60 days and was completed by 2,000 days. Additional experiments were conducted at temperatures of 50, 70, and 90 °C. As expected, the results show that the onset of hydration occurred much earlier at higher temperatures and hydration was completed sooner than in the 20 °C experiment.

A number of additional early studies of periclase hydration are summarized by Klemm (2005). The age of many of these studies make the acquisition of the original papers difficult. Thus, the discussion below is based on the summaries presented by Klemm (2005). The kinetics of MgO hydration in dolomitic limes at different temperatures was reported in Wells and Taylor (1937). They found that MgO was 95% hydrated in 40 minutes when placed in a 177 °C steam environment. At 25 °C it took about 75 days to achieve the same degree of hydration. Conversely, the results of an unpublished study are presented in Klemm (2005) in which a high-MgO clinker was used to prepare a cement paste. Bars made from this paste were stored under water for 31 years and at the end of this time slightly more than 40% of the original periclase content remained unhydrated. Because the original publications of the above articles were not available it is difficult to compare these older studies to the more recent ones described above. Numerous factors such as the composition of the cement and process used to prepare the clinkers (hard burned vs. dead burned) have a significant effect on the hydration characteristics of cements.

5.1.2 Natural Analogues

Periclase forms naturally in contact-metamorphosed dolomite and Mg-bearing limestone via the decarbonation reaction:



However, periclase is relatively scarce in the field because retrograde alteration and weathering result in essentially complete alteration of periclase to brucite (Turner, 1980; Bambauer et al., 1979). There are numerous well studied contact-metamorphic aureoles in marbles and the nearly ubiquitous absence of periclase in these terrains is evidence of the ability of periclase to rapidly hydrate. Some of the best studied aureoles are listed in Table 3. Of the 13 aureoles listed in this table only a few have reported the possible occurrence of primary periclase. The remaining studies have only observed brucite after periclase. It is important to note that the hydration of periclase to brucite in these contact-

metamorphic environments likely occurred as the metamorphic terrains cooled from their peak temperatures. The hydration temperatures would still have been elevated by several hundred degrees relative to the conditions at WIPP. However, these natural analogues do provide another line of evidence for the susceptibility of periclase to hydration.

5.1.3 Other Studies

A number of additional studies are described in the literature that supports the idea of rapid periclase hydration. Brandao et al. (2003) summarize the results of an extensive study on the mechanisms of carbonation and hydration in magnesia sinters (Brandao et al., 1998a) whose compositions were very similar to the Martin Marietta MgO used at WIPP. In these experiments magnesia sinters were crushed to a specific mesh size, spread evenly on metal trays and exposed to different environments. They found that magnesia sinters exposed to air under normal relative humidity formed rinds of hydromagnesite (5424) or a similar amorphous phase. However, in this environment little or no hydroxylation was observed. In a second experiment it was determined that if the sinters were exposed to air with simultaneous contact with liquid or vapor water then the formation of crystalline brucite with amorphous hydrated carbonates was observed. Finally, in experiments in which the sinters were exposed to water (liquid or vapor) but without initial contact to air, brucite was the only phase that formed. In another study, Brandao et al. (1998b) showed that the formation of brucite rinds surrounding the periclase grains does not inhibit the further growth of brucite. It was determined that diffusion of water vapor through the brucite crusts already formed can reach and consume the underlying periclase core. These experiments show the highly reactive nature of periclase in the natural environment. Even in the case where the periclase was initially passivated by a thin rind of hydromagnesite any subsequent contact with liquid or vapor water result in rapid consumption of the periclase to either hydromagnesite or brucite. This is further illustrated by the failed experiment discussed by Brandao et al. (2003). The purpose of this set of experiments was to determine what steps could be taken to hinder the degradation of the magnesia sinters during storage. In one of their experiments three samples of magnesia sinter were aged in a moist room for 52 days. At the end of the experiment hydromagnesite was the only phase observed in two of the samples, which is consistent with the earlier results. However, in the third sample set a small amount of brucite was found. During this experiment, a small amount of water condensed and came into contact with the magnesia sinter. This resulted in the formation of brucite in that part of the sample.

Finally, the susceptibility of periclase to hydration is illustrated by numerous experimental studies to define the brucite to periclase reaction at high pressure and temperature. Although the environmental conditions of these experiments are far above any conditions expected at WIPP they do provide some insight into the nature of periclase hydration. Typically in such experiments crystalline brucite is placed in an experimental capsule containing water. The capsule is then placed under pressures on the order of 500 to 10,000 atm and heated to temperatures of 600 °C and higher. After allowing the experiments to equilibrate for a period of time (days to weeks) the experiments are rapidly quenched to room temperature over a period of fractions of a second to a few minutes, depending on the experimental apparatus. The experiments are then opened to observe whether or not periclase formed. Unfortunately many of the experiments in the brucite-periclase system are plagued by almost complete back reaction of periclase to brucite during the quench even though it occurred almost instantaneously (Johannes and Metz, 1968; Franz, 1982). The reactivity of periclase is a well-known hindrance to these types of experiments and many researchers have tried novel methods to overcome the problem of rapid hydration (Schramke et al., 1982; Aranovich and Newton, 1996).

5.2 Brucite Carbonation

Studies of the carbonation of brucite to form hydromagnesite and eventually magnesite are not nearly as prevalent in the literature as those for periclase hydration. However, there are a number of interesting natural analogues discussed. The first set of reports stems from the CO₂-sequestration literature. There is a great deal of interest in the ability of brucite to carbonate because it is seen as a possible way in which to scrub anthropogenic CO₂ from the atmosphere, which occurs readily, or to use in power plants to prevent the release of CO₂ in the first place. In an online report, Herzog (2002) presents an overview and assessment of C sequestration via mineral carbonation. One of the processes reviewed in this report is the acid digestion of serpentine and subsequent precipitation of brucite by dehydration of the solution. It is then stated that brucite "can be readily reacted with CO₂." The process, however, is not seen as economically viable because of the energy needed to evaporate the solution and not due to the kinetics of brucite carbonation.

In addition to the CO₂ sequestration studies there are a number of natural analogues discussed in the literature. Most of these involve the weathering of serpentinite bodies. These bodies are formed due to the hydrous alteration of olivine-rich parent rocks into serpentine-rich rocks. Brucite also forms in the bodies during this initial serpentinization. A study of the New Idria serpentinite in California showed that brucite is a major constituent of the body (Mumpton and Thompson, 1966). This study found that brucite is abundant in the freshly exposed rock but is almost absent from the surface of the weathered zone, which persists to a depth of 20 to 30 feet across the entire body. In this weathered zone the brucite was transformed into pyroaurite (Mg₆Fe₂(CO₃)(OH)₁₆·4H₂O) and coalingite (Mg₁₀Fe₂(CO₃)(OH)₂₄·2H₂O). In other places the brucite was replaced by hydromagnesite. Similar results are also seen in serpentinite bodies at Atlin, British Columbia (Hansen et al., 2005) and the Xerolivadon region in Greece (Mposkos and Perdikatsis, 1986).

Finally, a study by Twilley (2006) investigated the weathering of an Indus Valley Culture carved statue. The statue dates to approximately 2000 B.C. and was carved from a type of rock known as predazzite, which is a brucite or periclase bearing limestone marble. The study clearly showed that the interior of the stone is composed almost entirely of calcite and brucite. However, on the exposed surfaces the brucite has been altered to hydromagnesite or magnesite. Of course, it is not known when the alteration of the brucite occurred in the nearly 4,000 year history of this statue. However, an important observation is made in the study. There are a number of areas on the statue with recent scarring due to impacts. Analysis of the surfaces of these recent surface exposures showed only the presence of calcite, hydromagnesite and magnesite. These results would suggest that the carbonation of brucite likely occurs on short (human) timescales.

5.3 Reconsideration of a Reported Instance of Long-Term Persistence of Hydromagnesite

We stated above that, based on extrapolations by Zhang et al. (2000) of data obtained at 110, 150, and 200 °C to 25 °C, over 99.9% of any (thermodynamically metastable) hydromagnesite in the WIPP would convert to (thermodynamically stable) magnesite after about 1000 years (see Subsection 4.1 above).

This conclusion is consistent with that reached by the EPA (U.S. EPA, 1998) during its review of the WIPP CCA (U.S. DOE, 1996). The EPA stated that:

“[T]he sequence of events resulting from brine infiltration and reaction with the MgO backfill in the repository may be conceptualized by the following reactions, in order:

1. Rapid reaction (hours to days) between the brine and MgO to produce brucite.
2. Rapid carbonation (hours to days) of the brucite to produce nesquehonite and possibly hydromagnesite.
3. Rapid conversion (days to weeks) of the nesquehonite to hydromagnesite.
4. Slow conversion (hundreds to thousands of years) of the hydromagnesite to magnesite”

However, the EPA also stated in the same document that:

“These estimates of conversion rate are confounded by the fact that deposits of hydromagnesite are found in some evaporite basins dated as late Quaternary in age (<23.7 million years) (Stamatakis, 1995), indicating that the hydromagnesite has persisted in a metastable state for a long period with only partial conversion to magnesite and other magnesium carbonates.”

Therefore, we reconsidered the paper by Stamatakis (1995) and concluded that: (1) it is not clear based on the poorly constrained age(s) of the huntite-hydromagnesite deposits in the Kozani Basin, Greece, that the hydromagnesite there has persisted longer than expected based on the results of Zhang et al. (2000); (2) it is unclear that any conclusions regarding the kinetics of the hydromagnesite-magnesite reaction based on the form of hydromagnesite present in the Kozani Basin are applicable to the conversion of the form of hydromagnesite produced in WIPP-relevant laboratory experiments.

Stamatakis (1995) reported various ages or ranges of ages for the huntite-hydromagnesite deposits in the Kozani Basin. He referred to the sedimentary rocks that host these deposits as “late Neogene” and, on two occasions, “uppermost Neogene.” He referred to the alkaline, saline, spring-fed lakes and ponds from which these evaporite deposits precipitated as “Tertiary to Recent” and “Neogene.” He did not provide any absolute (radiometric) ages for these deposits.

According to the current geologic time scale established by the International Commission on Stratigraphy, the Neogene Period has lasted from 23.03 Ma to the present (Gradstein et al., 2005). Therefore, the ages “Neogene,” “late Neogene,” “uppermost Neogene,” and “Tertiary to Recent” do not place a lower limit on the possible range of ages of these deposits, especially in the absence of absolute ages. Furthermore, the description of the deposits provided by Stamatakis (1995) is consistent with a postdepositional origin for at least some of the deposits, which further loosens any constraints on their ages. Therefore, it is not clear that the hydromagnesite there has persisted longer than expected based on the results of Zhang et al. (2000).

Furthermore, the hydromagnesite in the huntite-hydromagnesite deposits of the Kozani Basin is hydromagnesite (4323). There are at least two forms of hydromagnesite, one with the composition $Mg_4(CO_3)_3(OH)_2 \cdot 3H_2O$ and the other $Mg_5(CO_3)_4(OH)_2 \cdot 4H_2O$. In many of our analysis plans,

analysis reports, presentations, and publications, we have referred to the former as “hydromagnesite (4323)” and the latter as “hydromagnesite (5424).” Thermodynamic data for both of these forms of hydromagnesite are now in the EQ3/6 and FMT databases; these codes have always predicted that hydromagnesite (5424) will form under expected WIPP conditions instead of hydromagnesite (4323) if we suppress magnesite (i.e., prevent the more stable magnesite from forming at the expense of hydromagnesite (5424) by switching off magnesite in the input file). Moreover, we have consistently observed hydromagnesite (5424) in our laboratory studies of the carbonation of MgO under these conditions, but we have never observed hydromagnesite (4323). Finally, Zhang et al. (2000) used hydromagnesite (5424) in their study of the conversion of hydromagnesite to magnesite. Therefore, it is unclear that any conclusions regarding the rate of the hydromagnesite-to-magnesite reaction based on the hydromagnesite (4323) present in the Kozani Basin are applicable to the conversion of the hydromagnesite (5424) observed in our laboratory experiments and used by Zhang et al. (2000).

6 POSSIBLE CONSUMPTION OF CO₂ BY OTHER MATERIALS

The likelihood of and extent to which CO₂ will be consumed by other materials in the WIPP is important because these processes could increase the MgO effective excess factor and affect the evolution of chemical conditions in the near field of the repository. The types of materials or processes that could consume CO₂ (in addition to the MgO engineered barrier) are: (1) Fe-base metals in steel waste containers and in the TRU waste being emplaced in the repository, and the corrosion products of these metals; (2) Pb-base metals in the waste, and their corrosion products; (3) lime and portlandite in portland cements associated mainly with process sludges in the waste; (4) dissolution of CO₂ in WIPP brines; (5) incorporation of CO₂ in biomass; and (6) precipitation of carbonate minerals resulting from the reaction of CO₂ with dissolved Ca²⁺ that would be released to WIPP brines by the dissolution of SO₄²⁻-bearing minerals in the Salado Fm. surrounding the repository if after microbial SO₄²⁻ reduction in the repository consumes all SO₄²⁻ available in the waste. The possible consumption of CO₂ by the first five types of materials or processes is described in detail in this memorandum; consumption of CO₂ by precipitation of carbonate minerals is described in a separate analysis report.

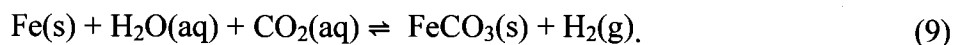
It is likely that these processes will consume significant quantities of CO₂ in addition to that consumed by MgO.

6.1 Iron-Base Metals and Their Corrosion Products

Metallic Fe in steel waste containers, the steel and other Fe-base metals in the TRU waste being emplaced in the WIPP, and the corrosion products of these metals could consume significant quantities of CO₂ in the repository. However, uncertainties remain as to whether and how much CO₂ they would consume. Brush (1990, 1995) and Wall and Enos (2006) reviewed thermodynamic and kinetic aspects of the chemical behavior of metallic Fe and Fe(II) corrosion products under expected WIPP conditions; Telander and Westerman (1993, 1997) carried out laboratory experiments to quantify the rates of H₂ production from anoxic corrosion of steels under these conditions. The following discussion summarizes the most important results of this work.

Telander and Westerman (1993, 1997) observed that steels reacted rapidly with CO₂ under brine-inundated conditions via the reaction:

Information Only



In Reaction 9, $\text{FeCO}_3\text{(s)}$ is the mineral siderite, which Telander and Westerman (1993) identified using XRD analysis.

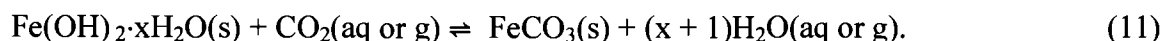
Reaction 9 proceeded rapidly, at least initially, because P_{CO_2} was high at the start of these experiments: ~ 12 atm in the “Excess CO_2 Tests” and ~ 0.39 - 7.8 atm in the “Controlled- CO_2 Addition Tests” (Telander and Westerman, 1997, Subsection 6.1.1.2, pp. 6-7 to 6-14). These values are several orders of magnitude higher than those expected in the WIPP, wherein the brucite-hydromagnesite carbonation reaction and – eventually – the brucite-magnesite carbonation reaction are expected to buffer P_{CO_2} at values of $\sim 10^{-5.5}$ or $10^{-6.9}$ atm, respectively (Brush, 2005). Telander and Westerman (1993, 1997) used high values of P_{CO_2} because they designed, started, and completed their experiments before the MgO engineered barrier was added to the WIPP disposal system.

In most cases, Reaction 9 ceased soon after the start of these experiments because of passivation of the steels caused by formation of an adherent layer of siderite (FeCO_3). In some cases, however, carbonation of steel continued because the initial quantity of CO_2 present in the experiments was insufficient to passivate the steels prior to sloughing off of corrosion products (compare the results of the “Immersed-Specimen Tests” in Figure 6-2 and those from Containers 33 and 34 in Figure 6-3, in which passivation did occur or was beginning to occur; with those from Containers 35-37 in Figure 6-3 of Telander and Westerman, 1997, in which passivation clearly did not occur). Sloughing probably occurred because the reaction:



produced nonadherent, crystalline, but unidentifiable $\text{Fe(OH)}_2 \cdot x\text{H}_2\text{O}$ similar in composition to amakinite (Fe(OH)_2) at rates greater than or equal to those of Reaction 9 in Containers 35-37 (Telander and Westerman, 1997, Figure 6-3). The corrosion product was unidentifiable because its XRD pattern was not present in any of the files available at the time that Telander and Westerman (1993, 1997) carried out their experiments. Other Fe(II)-bearing solid and aqueous corrosion products could also form in the WIPP, but the conclusions presented below do not depend on the identities of these aqueous species or solid phases, so other possible corrosion products will not be discussed here.

Of course, $\text{Fe(OH)}_2 \cdot x\text{H}_2\text{O}$ produced by Reaction 10 (and other Fe(II)-bearing corrosion products) could react with CO_2 produced subsequently by microbial activity in the WIPP. The carbonation reaction for the amakinite-like solid is:



There are at least three uncertainties pertaining to how much CO_2 could be consumed by carbonation of metallic Fe and Fe(II)-bearing corrosion products.

First, the size of the stability field of siderite is proportional to f_{CO_2} . Wall and Enos (2006) pointed out that the siderite stability field is very small at a total inorganic carbon (TIC) concentration of 10^{-4} M but is located very close to the Eh and pH expected in the WIPP, and that it expands as

the TIC increases to 10^{-3} and 10^{-2} M (see Figures 11 and 12 in Chivot, 2005). In the WIPP, anoxic corrosion of steels and other Fe-base metals will decrease the Eh to values at or below the lower stability limit of H₂O on an Eh-pH diagram; the pH buffered by the brucite dissolution reaction will be 8.69 in GWB and 8.94 in ERDA-6 (Brush, 2005). Because the TIC calculated by Brush (2005) in the FMT runs for the WIPP CRA-2004 Performance Assessment Baseline Calculations (PABC) is $\sim 3.50 \times 10^{-4}$ ($10^{-3.46}$) M in GWB and 4.28×10^{-4} ($10^{-3.37}$) M in ERDA-6, it is unclear that siderite will be stable enough in the repository for significant consumption of CO₂ by carbonation of metallic Fe and Fe(II)-bearing corrosion products. On the other hand, if for some unanticipated reason MgO fails to consume CO₂ as expected, or there is insufficient MgO available locally for some unexpected reason, the f_{CO_2} will increase, the stability field of siderite will expand, and carbonation via Reactions 10 and/or 11 will prevent the further increases in f_{CO_2} . Therefore, carbonation of metallic Fe and Fe(II)-bearing corrosion products could provide an effective “back-up” for carbonation of brucite and/or periclase.

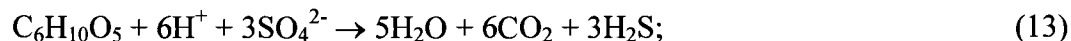
Second, the carbonation rates of these materials in WIPP brines have not been measured yet at values of P_{CO_2} approaching those predicted for the brucite-hydromagnesite and the brucite-magnesite carbonation reactions ($\sim 10^{-6.9}$ or $10^{-5.5}$ atm, respectively). Therefore, even if siderite is stable enough at these values of P_{CO_2} for significant carbonation to occur, it is unclear that it will form fast enough to consume significant quantities of CO₂ during the 10,000-year regulatory period.

Third, although passivation of steels and other Fe-base metals appears unlikely based on the results of Telander and Westerman (1997) (see above), it cannot be ruled out entirely yet.

The study of the corrosion of steels under expected WIPP conditions will address these and other uncertainties (Wall and Enos, 2006). However, it is already possible to calculate a conservative, minimum amount of CO₂ that could be consumed by carbonation of the steels and other Fe-base metals in the WIPP if: (1) siderite is stable enough under expected WIPP conditions for significant carbonation to occur, (2) the carbonation rates are high enough to consume significant quantities of CO₂ during the 10,000-year regulatory period; and (3) passivation of steels and other Fe-base metals does not occur. All of the inventory and other parameters used for this calculation (e.g., Crawford, 2005a; 2005b) are from the CRA-2004 PABC (Leigh et al., 2005), the current WIPP PA baseline.

The total moles of carbon (C) in the CPR materials to be emplaced in the WIPP is 1.10×10^9 mol. This value, which includes the CPR materials in the waste packaging materials, was obtained using: (1) the densities of cellulosic materials in contact-handled (CH) waste (60 kg/m^3) and remote-handled (RH) waste (9.3 kg/m^3), both from Crawford (2005b); (2) the densities of plastic materials in CH waste (43 kg/m^3), CH waste containers (17 kg/m^3), RH waste (8.0 kg/m^3), and RH waste containers (3.1 kg/m^3) (Crawford, 2005b); (3) a factor of 1.7 used multiply the densities of the plastic materials to account for the additional C content of these materials relative to those of cellulosic and rubber materials (Wang and Brush, 1996); (4) the densities of rubber materials in CH waste (13 kg/m^3) and RH waste (6.7 kg/m^3); (5) the total volumes of CH waste ($168,485 \text{ m}^3$) and RH waste ($7,079 \text{ m}^3$) to be emplaced in the WIPP; and (6) the molecular weight of cellulose (C₆H₁₀O₅) (162.1436 g/mol).

The total moles of CO₂ and H₂S produced by complete microbial consumption of the CPR materials in the WIPP are 1.10×10^9 mol CO₂ and 5.24×10^8 mol H₂S. This value was obtained from: (1) the total moles of C in the CPR materials to be emplaced in the WIPP (1.10×10^9 mol); (2) the overall reactions for microbial denitrification and microbial SO₄²⁻ reduction from Wang and Brush (1996):



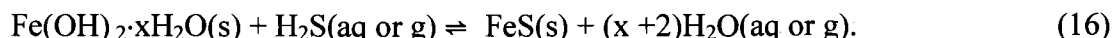
(3) use of the quantity of NO_3^- in the PABC inventory (Crawford, 2005a) to calculate that, if microorganisms consume all CPR materials in the repository, denitrification will consume 4.89% of the CPR materials and SO_4^{2-} reduction will consume the remaining 95.1%. Use of the assumption that microbial methanogenesis,



will not occur in the WIPP has been specified by the EPA since it approved the disposal of supercompacted waste in the WIPP in 2004 (Marcinowski, 2004). This results in a CO_2 yield of 1 mole/mole C instead of a yield close to 0.5 that would be obtained if 4.89% of the CPR materials were consumed by denitrification, 0.837% by SO_4^{2-} reduction using only the SO_4^{2-} in the waste and no naturally occurring SO_4^{2-} , and 94.3 % by methanogenesis.

The total moles of metallic Fe in the steel waste containers, and the steel and other Fe-base metals in the TRU waste being emplaced in the WIPP is 9.21×10^8 moles. This was obtained using (1) the densities of metallic Fe in CH waste containers (170 kg/m^3), CH waste (110 kg/m^3), RH waste containers (540 kg/m^3), and RH waste (59 kg/m^3), all from Crawford (2005b); (2) the total volumes of CH waste ($168,485 \text{ m}^3$) and RH waste ($7,079 \text{ m}^3$) to be emplaced in the WIPP; and (3) the molecular weight of Fe (55.845 g/mole).

Metallic Fe and Fe(II)-bearing corrosion products in the WIPP will probably consume H_2S preferentially to CO_2 via reactions such as:



Telander and Westerman (1993, 1997) observed the formation of mackinawite (Fe_{1-x}S) from corrosion of steels in their experiments, but the nonstoichiometric composition of this corrosion product is neglected here for simplicity. Furthermore, mackinawite passivated the steels in their experiments. However, $P_{\text{H}_2\text{S}}$ was several orders of magnitude higher in these experiments than it will be in the WIPP, because microbial SO_4^{2-} reduction will proceed at very low rates relative to those of sulfidization of steels and corrosion products such as $\text{Fe(OH)}_2 \cdot x\text{H}_2\text{O}$. Therefore, sloughing off of $\text{Fe(OH)}_2 \cdot x\text{H}_2\text{O}$ produced by Reaction 10 (see above), which will not be rate-limited by the production of a reactant such as H_2S if there is sufficient brine present for microbial activity, will probably prevent passivation of steels by mackinawite in the repository.

However, sulfidization of metallic Fe and its corrosion products (Reactions 15 and 16) will occur preferentially to carbonation (Reactions 9 and 11) because: (1) the values of $P_{\text{H}_2\text{S}}$ required to stabilize sulfides such as mackinawite are several orders of magnitude lower than the values of P_{CO_2} required to stabilize carbonates such as siderite (see, for example, Brush, 1990; Wall and Enos, 2006), and (2) the moles of H_2S that would be produced by microbial consumption of all CPR materials

(5.24×10^8 mol) is within one order of magnitude of the moles of CO_2 so produced (1.10×10^9 mol). Therefore, calculation of a conservative, minimum amount of CO_2 that could be consumed by carbonation of the steels and other Fe-base metals in the WIPP must first assume that all microbially produced H_2S will react with metallic Fe and its corrosion products to produce mackinawite. Of course, a significantly nonstoichiometric mackinawite composition (equivalent to a large value of x in a Fe_{1-x}S), production of pyrite (FeS_2), or reaction of H_2S with other metals (e.g., Pb) would increase the CO_2 uptake capacity of steels, other Fe-base metals, and their corrosion products to values above the minimum value (see below).

Thus, the minimum quantity of CO_2 that could be consumed by carbonation of steels and other Fe-base metals (or their corrosion products) if the three conditions described above are met is 3.97×10^8 mol, obtained by subtracting 5.24×10^8 mol of FeS from the 9.21×10^8 mol of metallic Fe to be emplaced in the repository. This minimum CO_2 uptake capacity is 36.1% of the CO_2 that would be produced by complete microbial consumption of all CPR materials in the repository.

6.2 Lead-Base Metals and Their Corrosion Products

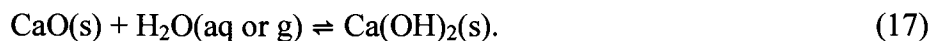
Metallic Pb in the TRU waste being emplaced in the WIPP could behave similarly in many respects to the steels and other Fe-base metals being emplaced (Wall and Enos, 2006). In particular, corrosion of Pb-base metals could result in corrosion products analogous or nearly analogous to those of steels, other Fe-base metals, and their corrosion products. These Pb-bearing corrosion products include cerussite (PbCO_3) and galena (PbS). On the other hand, the behavior of Pb-base metals in the WIPP is also subject to uncertainties similar to those described above for Fe-base metals, but there have been no studies of the behavior of Pb-base metals under expected WIPP conditions yet.

Wall and Enos (2006, p. 38) estimated the minimum quantity of metallic Pb to be emplaced in the WIPP at 3.0×10^6 kg, or 1.5×10^7 mol. This estimate is based on the densities of Pb in CH and RH TRU waste provided for the PABC by Crawford (2005b, 2005c). If all H_2S produced by microbial consumption of all CPR materials in the WIPP were consumed by sulfidization of steels and other Fe-base metals (or their corrosion products), the moles of CO_2 that could be consumed by carbonation of Pb would be 1.5×10^7 mol. This is 3.78% of the quantity that could be consumed by carbonation of steels, other Fe-base metals, or their corrosion products, and 1.36% of the CO_2 that would be produced by complete microbial consumption of all CPR materials in the repository.

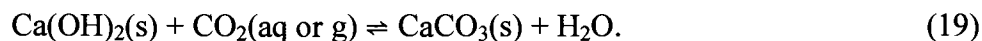
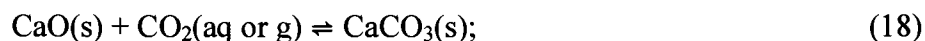
On the other hand, sulfidization of metallic Pb and its corrosion products could occur prior to sulfidization of metallic Fe and its corrosion products. This is because the solubility product of galena is much lower than that of mackinawite or pyrrhotite (FeS). In the compilations of Sillén and Martel (1964, 1971), the log of the solubility product ($\log K_{sp}$) of galena is -27.47, whereas $\log K_{sp}$ of the latter is -18.43. Sillén and Martel (1964, 1971) did not specify whether "FeS" refers to mackinawite, pyrrhotite, or some other FeS polymorph, but the difference between $\log K_{sp}$ of galena and FeS is so great that it probably doesn't matter which polymorph the $\log K_{sp}$ of -18.43 pertains to. In any case, galena is so much more stable than FeS that, if H_2S , HS^- , and S^{2-} are present, the reduced sulfur would likely be consumed by metallic Pb or its corrosion products prior to sulfidization of metallic Fe or its corrosion products. If so, the quantity of CO_2 consumed by metallic Fe and its corrosion products would increase from 36.1% to 37.46%, or about 37.5%, of the CO_2 that would be produced by complete microbial consumption of all CPR materials in the repository.

6.3 Lime and/or Portlandite in Portland Cements

Lime is present in the Portland cement used by the waste generators to dewater process sludges prior to shipment to the WIPP. This is because the WIPP Waste Acceptance Criteria require that free liquids constitute no more than 1 vol % of the waste. Dewatering of the sludges results in the hydration of some, but not all, of the lime, which forms portlandite:



Carbonation of lime and portlandite produces calcite, which forms much faster than hydromagnesite or magnesite:



Ca sulfides are not stable under the conditions expected in the WIPP.

The total quantity of free lime in the Portland cements used to dewater the process sludges to be emplaced in the WIPP is 1.95×10^6 mol. This value was obtained from: (1) the total mass of Portland cement to be emplaced in the repository (8.80×10^6 kg), from Howard (2005, Table 7); (2) the concentration of free lime in Portland cement (1.243 wt %), from Lawrence (1998, pp. 135-138); and (3) the molecular weight of CaO (56.0794 g/mol).

“Free” lime refers to the CaO not incorporated in the compounds created when Portland cement hydrates to make concrete, such as the Ca-Si oxides Ca_3SiO_5 and Ca_2SiO_4 , the Ca-Al oxide $\text{Ca}_3\text{Al}_2\text{O}_6$, and the Ca-aluminoferrite solid solution $x\text{Ca}_2\text{Al}_2\text{O}_5 \cdot y\text{Ca}_2\text{Al}_2\text{O}_5$ (see, for example, Lawrence, 1998). The average concentration of free lime in Portland cement (1.243 wt %) from Lawrence (1998, pp. 135-138) is the average free-lime content of about 200-300 Portland cements “including data from a number of countries throughout the world.” Lawrence did not provide the total number of Portland cements analyzed to obtain his average free-lime content of 1.243% given in his Table 4.1, but inspection of the histograms in his Figures 3.1 through 4.3, which provided other average chemical properties of Portland cements, reveal that he included about 200-300 analyses. We will use this value instead of Storz’s (1996) estimate of 10% for the free-lime content for the WIPP CCA PA, because Storz estimated 10% without any supporting data, and apparently estimated an unrealistically high value to be conservative in the absence of any data.

Carbonation of the free lime in the Portland cements used to dewater the process sludges to be emplaced in the WIPP will consume 1.95×10^6 mol of CO_2 . This is 0.491% of the quantity that could be consumed by carbonation of steels and other Fe-base metals or their corrosion products, and 0.177% of the CO_2 that would be produced by complete microbial consumption of all CPR materials in the repository.

6.4 Dissolution of CO₂ in WIPP Brines

Dissolution of CO₂ in WIPP brines cannot consume significant quantities of CO₂ relative to the quantity that would be produced by microbial consumption of all CPR materials in the repository. This is because the solubility of CO₂ in brines is too low, and the volumes of brines that could flow through the repository are too low to dissolve significant amounts of CO₂. The CO₂ solubility is too low because the brucite-magnesite or brucite-hydromagnesite carbonation reactions will buffer f_{CO_2} at values of $10^{-6.9}$ or $10^{-5.5}$ atm, respectively.

The total dissolved CO₂ concentrations in GWB and ERDA-6 calculated by FMT for the PABC are 3.50×10^{-4} and 4.28×10^{-4} M, respectively (Brush, 2005, Runs 7 and 11). The five dissolved CO₂ species with the highest concentrations in GWB are MgCO₃(aq) (2.42×10^{-4} M), HCO₃⁻ (4.22×10^{-5} M), CO₃²⁻ (2.16×10^{-5} M), CaCO₃(aq) (3.64×10^{-6} M), and NpO₂CO₃⁻ (1.04×10^{-7} M). The five most important dissolved CO₂ species in ERDA-6 are MgCO₃(aq) (2.79×10^{-4} M), HCO₃⁻ (7.90×10^{-5} M), CO₃²⁻ (5.18×10^{-5} M), CaCO₃(aq) (1.72×10^{-5} M), and NpO₂CO₃⁻ (4.08×10^{-7} M).

The minimum volume of brine in the repository required for a brine release is 10,011 m³ (Stein, (2005). Multiplication of 10,011 m³ of GWB by 10³ L/m³ and 3.50×10^{-4} M total dissolved CO₂ yields a total of 3.50×10^3 moles of CO₂ in 10,011 m³ of GWB. The total dissolved CO₂ concentration of ERDA-6 is higher than that of GWB, and larger volumes of ERDA-6 could flow through the WIPP in the event of human intrusions that penetrate a brine reservoir in the Castile Fm., which underlies the Salado. Larger volumes of brine would, of course, contain more dissolved CO₂: 100,000 m³ of ERDA-6 would contain $100,000 \text{ m}^3 \times 10^3 \text{ L/m}^3 \times 4.28 \times 10^{-4} \text{ M} = 4.28 \times 10^4$ moles of CO₂, and 1,000,000 m³ would contain 10 times this amount or 4.28×10^5 moles of CO₂. Nevertheless all these quantities of CO₂ are miniscule compared to the quantity that would be produced by microbial consumption of all CPR materials in the repository, 1.10×10^9 moles. In fact, the amounts of CO₂ dissolved in 10,011 m³ of GWB, 100,000 m³ of ERDA-6, or 1,000,000 m³ of ERDA-6 are just 0.000318%, 0.00389%, and 0.0389%, respectively, of the total quantity of CO₂ that would be produced by microbial consumption of all CPR materials in the repository.

6.5 Incorporation of CO₂ in Biomass

Some of the organic C in CPR materials would be sequestered in biomass (cellular material) instead of being oxidized to CO₂ if significant microbial consumption of these materials occurs in the WIPP. However, it would be difficult to predict defensibly how much C would be sequestered in biomass. For example, the mass of biomass would probably decrease after microorganisms consume all CPR materials. Microorganisms existing at that time would die, become dormant, or produce resistant forms (e.g., spores) that could remain viable for potentially long periods. Furthermore, some of the microbes existing after consumption of all CPR materials could consume dead or dormant microbes, thereby decreasing the mass of biomass.

Because of potential difficulties in calculating and defending the mass and ultimate fate of biomass in the WIPP, we cannot quantify this uncertainty in the MgO effective excess factor. However, exclusion of biomass from the excess factor could be at least slightly conservative.

6.6 Implications for the MgO Effective Excess Factor

Inclusion of the effects of consumption of CO₂ by Fe-base metals and their corrosion products, Pb-base metals and their corrosion products, and CaO and Ca(OH)₂ in Portland cement would be difficult at present because of the uncertainties associated with these processes in the WIPP (see Subsection 5.1, 5.2, and 5.3 above). However, these materials could consume 36.1, 1.36, and 0.177% of the CO₂ that would be produced by complete microbial consumption of all CPR materials in the repository.

7 CONCLUSIONS

Incorporation of the effect of the concentrations of reactive constituents in Premier and Martin Marietta MgO in the MgO effective excess factor necessitates multiplication of the excess factor by 0.89 and 0.96, respectively. Premier MgO contains ~89 mol % (92 wt %) periclase and lime (see Table 1 above). Martin Marietta MgO contains 96 mol % periclase (Tables 1 and 2).

All results to date imply that the periclase and lime present in MgO will be available to react – and will continue to react - until all CO₂ in the repository has been consumed. Therefore, the MgO effective excess factor need not be reduced to account for incomplete reaction, which is consistent with multiplication of the excess factor by 1.

Incorporation of the ratio of the number of moles of CO₂ consumed per mole of periclase in MgO into the effective excess factor necessitates multiplication of this factor by a value close to 1. The number of moles of CO₂ consumed per mole of periclase will be close to 1 because magnesite will be the dominant Mg carbonate throughout most of the 10,000-year regulatory period, and formation of magnesite will consume 1 mol of CO₂ per mol of periclase. The exact ratio of CO₂ consumed per mole of periclase will depend on how much CO₂ is produced by microbial activity prior to 9,000 years.

A review of the literature on MgO hydration under expected WIPP conditions, anthropogenic analogs, and natural analogs implies that periclase will hydrate if H₂O is present, and that brucite will carbonate if CO₂ is present.

Inclusion of the effects of consumption of CO₂ by Fe-base metals and their corrosion products, Pb-base metals and their corrosion products, and CaO and Ca(OH)₂ in Portland cement would be difficult because of the uncertainties associated with these processes. However, these materials could consume 36.1, 1.36, and 0.177% of the CO₂ that would be produced by complete microbial consumption of all CPR materials.

8 REFERENCES

Adams, J.E. 1944. "Upper Permian Ochoa Series of Delaware Basin, West Texas and Southeastern New Mexico," *American Association of Petroleum Geologists Bulletin*, Vol. 28, 1596-1625.

Information Only

- Aranovich, L. Ya., and R.C. Newton. 1996. "H₂O Activity in Concentrated NaCl Solutions at High Pressures and Temperatures Measured by Brucite-Periclase Equilibrium," *Contributions to Mineralogy and Petrology*. Vol. 125, 200–212.
- ASTM. 2005. *Standard Specification for Portland Cement*, ASTM C 150-05, American Society for Testing and Materials International: West Conshohocken, PA.
- Babb, S.C., and C.F. Novak. 1995. "WIPP PA User's Manual for FMT, Version 2.0." Albuquerque, NM: Sandia National Laboratories. ERMS 228119.
- Babb, S.C., and C.F. Novak. 1997 and addenda. "User's Manual for FMT Version 2.3: A Computer Code Employing the Pitzer Activity Coefficient Formalism for Calculating Thermodynamic Equilibrium in Geochemical Systems to High Electrolyte Concentrations." Albuquerque, NM: Sandia National Laboratories. ERMS 243037.
- Bambauer, H.U., F. Taborszky, and H.D. Trochim. 1979. *Optical Determination of Rock-Forming Minerals*. Stuttgart: E. Schweizerbart'sche Verlagsbuchhandlung.
- Bates, R.L., and J.A. Jackson, eds. 1984. *Dictionary of Geological Terms*, Third Edition. New York, NY: Anchor Books (Doubleday).
- Bowman, J.R., and E.J. Essene. 1982. "P-T-X(CO₂) Conditions of Contact Metamorphism in the Black Butte Aureole, Elkhorn, Montana," *American Journal of Science*. Vol. 282, 311-340.
- Bowman, J.R., and E.J. Essene. 1984. "Contact Skarn Formation at Elkhorn, Montana. I. P-T-component Activity Conditions of Early Skarn Formation," *American Journal of Science*, Vol. 284, 597-650.
- Brandao, P.R.G., G.E. Goncalves, and A.K. Duarte. 1998a. "Mechanisms of Hydration/Carbonation of Basic Refractories," *Refractories Applications and News*. Vol. 3, 6–9.
- Brandao, P.R.G., G.E. Goncalves, and A.K. Duarte. 1998b. "Mechanisms of Hydration/Carbonation of Basic Refractories Part II – Investigation of the Kinetics of Formation of Brucite in Fired Basic Bricks," *Refractories Applications and News*. Vol. 3, 9-11.
- Brandao, P.R.G., G.E. Goncalves, and A.G. Morato. 2003. "Mechanisms of Hydration/Carbonation of Magnesia Sinters – Part III," *Refractories Applications and News*. Vol. 8, 23–26.
- Brush, L.H. 1990. *Test Plan for Laboratory and Modeling Studies of Repository and Radionuclide Chemistry for the Waste Isolation Pilot Plant*. SAND90-0266. Albuquerque, NM: Sandia National Laboratories.
- Brush, L.H. 1995. "Systems Prioritization Method - Iteration 2 Baseline Position Paper: Gas Generation in the Waste Isolation Pilot Plant." March 17, 1995. Albuquerque, NM: Sandia National Laboratories. ERMS 228740.
- Brush, L.H. 2005. "Results of Calculations of Actinide Solubilities for the WIPP Performance Assessment Baseline Calculations." Analysis report, May 18, 2005. Carlsbad, NM: Sandia National Laboratories. ERMS 539800.

- Brush, L.H., and Y. Xiong. 2003a. "Calculation of Actinide Solubilities for the WIPP Compliance Recertification Application, Analysis Plan AP-098, Rev. 1." Carlsbad, NM: Sandia National Laboratories. ERMS 527714.
- Brush, L.H., and Y. Xiong. 2003b. "Calculation of Actinide Solubilities for the WIPP Compliance Recertification Application." Analysis report, May 8, 2003. Carlsbad, NM: Sandia National Laboratories. ERMS 529131.
- Brush, L.H., and Y.-L. Xiong, 2005. "Calculation of Actinide Solubilities for the WIPP Performance Assessment Baseline Calculations, Analysis Plan AP-120, Rev. 0. April 4, 2005. Carlsbad, NM: Sandia National Laboratories. ERMS 539255.
- Bryan, C.R., and A.C. Snider. 2001a. "MgO Hydration and Carbonation at SNL/Carlsbad," "Sandia National Laboratories Technical Baseline Reports; WBS 1.3.5.4, Repository Investigations; Milestone RI010; January 31, 2001." Carlsbad, NM: Sandia National Laboratories. ERMS 516749. 66-83.
- Bryan, C.R., and A.C. Snider. 2001b. "MgO Experimental Work Conducted at SNL/CB: Continuing Investigations with Premier Chemicals MgO," "Sandia National Laboratories Technical Baseline Reports; WBS 1.3.5.4, Repository Investigations; Milestone RI020; July 31, 2001." Carlsbad, NM: Sandia National Laboratories. ERMS 518970. 5-1 to 5-15.
- Burnham, C.W. 1959. "Contact Metamorphism of Magnesian Limestones at Crestmore, California," *Geological Society of America Bulletin*. Vol. 70, 879-920.
- Carpenter, A.B. 1967. "A Mineralogy and Petrology of the System CaO-MgO-SiO₂-CO₂-H₂O at Crestmore, California," *American Mineralogist*, Vol. 52, 1341-1363.
- Chivot, J. 2005. Thermodynamique des Produits de Corrosion: Fonctions Thermodynamiques, Diagrammes de Solubilité, Diagrammes E-pH des Systèmes Fe-H₂O, Fe-CO₂-H₂O, Fe-S-H₂O, Cr-H₂O, et Ni-H₂O en Fonction de la Température. Collection Sciences et Techniques. Châtenay-Malabry, France: Agence National pour la Gestion des Déchets Radioactifs.
- Crawford, B.A. 2005a. "Determination of Waste Stream Oxyanions using TWBID Revision 2.1, Version 3.13, Data Version 4.15." Analysis report, February 24, 2005. Carlsbad, NM: Los Alamos National Laboratory. ERMS 538811.
- Crawford, B.A. 2005b. "Waste Material Densities in TRU Waste Streams from TWBID Revision 2.1, Version 3.13, Data Version D.4.15." Analysis report, April 13, 2005. Carlsbad, NM: Los Alamos National Laboratory. ERMS 539323.
- Crawford, B.A. 2005c. "Tables Containing Lead Data from TWBID Rev. 2-1 D4.15." Memorandum to J. Trone, October 20, 2005. Carlsbad, NM: Los Alamos National Laboratory. ERMS 541735.
- Daveler, S.A., and T.J. Wolery. 1992. *EQPT, A Data File Preprocessor for the EQ3/6 Software Package: User's Guide and Related Documentation (Version 7.0)*. UCRL-MA-110662 PT II. Livermore, CA: Lawrence Livermore National Laboratory.

- Deng, H., S. Johnsen, G. Roselle, and M. Nemer. 2006a. "Analysis of Martin Marietta MagChem 10 WTS-60 MgO." Analysis report, November 14, 2006. Carlsbad, NM: Sandia National Laboratories. ERMS 544712.
- Deng, H., M.B. Nemer, and Y. Xiong. 2006b. "Experimental Study of MgO Reaction Pathways and Kinetics, Rev. 0." TP 06-03, Rev. 0, June 6, 2006. Carlsbad, NM: Sandia National Laboratories. ERMS 543633.
- Ferry, J.M. 1989. "Contact Metamorphism of Roof Pendants at Hope Valley, Alpine County, California, USA: A Record of the Hydrothermal System of the Sierra Nevada Batholith," *Contributions to Mineralogy and Petrology*. Vol. 101, 402-417.
- Ferry, J.M. 1996. "Prograde and Retrograde Fluid Flow during Contact Metamorphism of Siliceous Carbonate Rocks from the Ballachulish Aureole, Scotland," *Contributions to Mineralogy and Petrology*. Vol. 124, 235--254.
- Ferry, J.M., and D. Rumble III. 1997. "Formation and Destruction of Periclase by Fluid Flow in Two Contact Aureoles," *Contributions to Mineralogy and Petrology*. Vol. 128, 313-334.
- Ferry, J.M., B.A. Wing, S.C. Penniston-Dorland, and D. Rumble III. 2002. "The Direction of Fluid Flow during Contact Metamorphism of Siliceous Carbonate Rocks: New Data for the Monzoni and Predazzo Aureoles, Northern Italy, and a Global Review," *Contributions to Mineralogy and Petrology*. Vol. 142, 679-699.
- Franz, G. 1982. "The Brucite-Periclase Equilibrium at Reduced H₂O Activities: Some Information about the System H₂O-NaCl," *American Journal of Science*. Vol. 282, 1325-1339.
- Garber, R.A., P.M. Harris, and J.M. Borer. 1990. "Occurrence and Significance of Magnesite in Upper Permian (Guadalupian) Tansil and Yates Formations, Delaware Basin, New Mexico," *American Association of Petroleum Geologists Bulletin*. Vol. 74, no. 2, 119-134.
- Gerdes, M.L., L.P. Baumgartner, and J.W. Valley. 1999. "Stable Isotopic Evidence for Limited Fluid Flow through Dolomitic Marble in the Adamello Contact Aureole, Cima Uzza, Italy," *Journal of Petrology*. Vol. 40, 853-872.
- Gradstein, F.M., J.G. Ogg, and A.G. Smith, Eds. 2005. *A Geologic Timescale 2004*. Cambridge, UK: Cambridge University Press.
- Hansen, L.D., G.M. Dipple, T.M. Gordon, and D.A. Kellett. 2005. "Carbonated Serpentinite (Listwanite) at Atlin, British Columbia: A Geological Analogue to Carbon Dioxide Sequestration," *Canadian Mineralogist*. Vol. 43, 225-239.
- Herzog, H. 2002. *Carbon Sequestration via Mineral Carbonation: Overview and Assessment*. Carbon Capture and Sequestration Technologies Program, Massachusetts Institution of Technology, Cambridge, <http://sequestration.mit.edu/pdf/carbonates.pdf>.
- Howard, B.A. 2005. "Estimate of Portland Cement in TRU Waste for Disposal in WIPP Based on TWBID Revision 2.1, Version 3.13, Data Version 4.15 (LA-UR-05-1733)." Analysis report, April 4, 2005. Carlsbad, NM: Los Alamos National Laboratory. ERMS 539241.

- Johannes, W., and P. Metz. 1968. "Experimentelle Bestimmung von Gleichgewichtsbeziehungen im System MgO-CO₂-H₂O," *Neues Jahrbuch für Mineralogie, Abhandlungen*. Vol. 112, 15-26.
- Kasselouris, V., C. Ftikos, and G. Parissakis. 1985. "On the Hydration of MgO in Cement Pastes Hydrated up to 8 Years," *Cement and Concrete Research*. Vol. 15, 758-764.
- Kerrick, D.M., K.E. Crawford, and A.F. Randazzo. 1973. "Metamorphism of Calcareous Rock in Three Roof Pendants in the Sierra Nevada, California," *Journal of Petrology*. Vol. 14, 303-325.
- Klemm, W.A. 2005. *Cement Soundness and the Autoclave Expansion Test – An Update of the Literature*. R&D Serial No. 2651. Skokie, IL: Portland Cement Association,
- Kozak, P.K., De.F. Duke, and G.T. Roselle. 2004. "Mineral Distribution in Contact-Metamorphosed Siliceous Dolomite at Ubehebe, California, Based on Airborne Imaging Spectrometer Data," *American Mineralogist*. Vol. 89, 701-713.
- Lang, W.B. 1939. "Salado Formation of the Permian Basin," *American Association of Petroleum Geologists Bulletin*. Vo. 23, 1569-1572.
- Lawrence, C.D. 1998. "The Constitution and Specification of Portland Cements," *Lea's Chemistry of Cement and Concrete*, Fourth Edition. Ed. P.C. Hewlett. London, UK: Arnold. 131-193.
- Leigh, C.D., J.F. Kanney, L.H. Brush, J.W. Garner, G.R. Kirkes, T. Lowry, M.B. Nemer, J.S. Stein, E.D. Vugrin, S. Wagner, and T.B. Kirchner. 2005. "2004 Compliance Recertification Application Performance Assessment Baseline Calculation, Revision 0. Analysis report, October 19, 2005. Carlsbad, NM: Sandia National Laboratories. ERMS 541521.
- Lowenstein, T.K. 1983. "Deposition and Alteration of an Ancient Potash Evaporite: The Permian Salado Formation of New Mexico and West Texas." Ph.D. dissertation. Baltimore, MD: The Johns Hopkins University.
- Lowenstein, T.K. 1988. "Origin of Depositional Cycles in a Permian 'Saline Giant': The Salado (McNutt Zone) Evaporites of New Mexico and Texas," *Geological Society of America Bulletin*. Vol. 100, 592-608.
- Marcinowski, F. 2004. Untitled letter with attachments from F. Marcinowski to R.P. Detwiler approving the DOE's request to dispose of compressed (supercompacted) waste from the Advanced Mixed Waste Treatment Program in the WIPP, March 26, 2004. Washington, DC: U.S. Environmental Protection Agency Office of Air and Radiation. ERMS 534327.
- Martin Marietta Magnesia Specialties. 2006. "Everything You Ever Wanted to Know about Magnesium Oxide." Downloaded from www.magspecialties.com/students.htm on November 14, 2006. ERMS 544711.
- Masch, L., and S. Heuss-Aßbichler. 1991. "Decarbonation Reactions in Siliceous Dolomites and Impure Limestones." G. Voll, J. Topel, D.R.M. Pattison, and F. Seifert, Eds. *Equilibrium and Kinetics in Contact Metamorphism: The Ballachulish Igneous Complex and Its Aureole*. Berlin, Germany: Springer Verlag.

- Moody, D.C. 2006. Untitled letter from D.C. Moody to E.A. Cotsworth requesting EPA approval of the DOE's request reduce the amount of excess MgO currently being emplaced in the WIPP, April 10, 2006. Carlsbad, NM: U.S. Department of Energy Carlsbad Field Office. ERMS 543262.
- Moore, J.N., and D.M. Kerrick. 1976. "Equilibria in Siliceous Dolomites of the Alta Aureole, Utah," *American Journal of Science*. Vol. 276, 502-524.
- Mposkos, E., and V. Perdikatsis. 1986. "Alteration of Brucite and Formation of Pyroaurite in Dunitic Serpentine in the Xerolivadon Region, Southern Vourinos," *Geologikai kai Geofysikai Meletai*. Special Volume, 279-285.
- Mumpton, F.A., and C.S. Thompson. 1966. "The Stability of Brucite in the Weathering Zone of the New Idria Serpentine," *Clays and Clay Minerals*. Vol. 14, 249-257.
- Munson, D.E., R.L. Jones, D.L. Hoag, and J.R. Ball. 1987. *Heated Axisymmetric Pillar Test (Room H): In Situ Data Report (February, 1985 - April, 1987), Waste Isolation Pilot Plant (WIPP) Thermal/Structural Interactions Program*. SAND87-2488. Albuquerque, NM: Sandia National Laboratories.
- Novak, C.F., R.C. Moore, and R.V. Bynum. 1996. "Prediction of Dissolved Actinide Concentrations in Concentrated Electrolyte Solutions: A Conceptual Model and Model Results for the Waste Isolation Pilot Plant (WIPP)." Unpublished presentation at the 1996 International Conference on Deep Geological Disposal of Radioactive Waste, September 16-19, 1996, Winnipeg, Manitoba, Canada. ERMS 418098, SAND96-2695C.
- Øvereng, O. 2000. "Granåsen, a Dolomite-Brucite Deposit with Potential for Industrial Development," *Norges Geologiske Undersøkelse Bulletin*. Vol. 436, 75-84.
- Oversby, V.M. 2000. *Plutonium Chemistry under Conditions Relevant for WIPP Performance Assessment: Review of Experimental Results and Recommendations for Future Work*. EEG-77. Albuquerque, NM: Environmental Evaluation Group.
- Popielak, R.S., R.L. Beauheim, S.R. Black, W.E. Coons, C.T. Ellingson and R.L. Olsen. 1983. *Brine Reservoirs in the Castile Formation, Waste Isolation Pilot Plant Project, Southeastern New Mexico*. TME 3153. Carlsbad, NM: U.S. Department of Energy WIPP Project Office.
- Qing, Y., C. Huxing, W. Yuqing, W. Shangkian, and L. Zonghan. 2004. "Effect of MgO and Gypsum Content on Long-term Expansion of Low Heat Portland Slag Cement with Slight Expansion," *Cement and Concrete Composites*. Vol. 26, 331-337.
- Roselle, G.T. 1997. *Integrated Petrologic, Stable Isotopic, and Statistical Study of Fluid-Flow in Carbonates of the Ubehebe Peak Contact Aureole, Death Valley National Park, California*. Ph.D. Dissertation. Madison, WI: University of Wisconsin-Madison.
- Roselle, G.T., L.P. Baumgartner, and J.W. Valley. 1999. "Stable Isotope Evidence of Heterogeneous Fluid Infiltration at the Ubehebe Peak Contact Aureole, Death Valley National Park, California", *American Journal of Science*. Vol. 299, 93-138.

- Schramke, J.A., D.M. Kerrick, and J.G. Blencoe. 1982. "Experimental Determination of the Brucite = Periclase + Water Equilibrium with a New Volumetric Technique," *American Mineralogist*. Vol. 67, 269–276.
- Sillén, L.G., and A.E. Martell. 1964. *Stability Constants of Metal-Ion Complexes*. London, UK: The Chemical Society. Special Publication No. 17.
- Sillén, L.G., and A.E. Martell. 1971. *Stability Constants of Metal-Ion Complexes*. London, UK: The Chemical Society. Special Publication No. 25.
- SNL. 1997. "Chemical Conditions Model: Results of the MgO Backfill Efficacy Investigation." April 23, 1997. Albuquerque, NM: Sandia National Laboratories. ERMS 419794.
- Snider, A.C. 2002. "MgO Studies: Experimental Work Conducted at SNL/Carlsbad. Efficacy of Premier Chemicals MgO as an Engineered Barrier," "Sandia National Laboratories Technical Baseline Reports; WBS 1.3.5.3, Compliance Monitoring; WBS 1.3.5.4, Repository Investigations; Milestone RI110; January 31, 2002." Carlsbad, NM: Sandia National Laboratories. ERMS 520467. 3.1-1 to 3.1-18.
- Snider, A.C. 2003a. "Hydration of Magnesium Oxide in the Waste Isolation Pilot Plant," "Sandia National Laboratories Technical Baseline Reports; WBS 1.3.5.3, Compliance Monitoring; WBS 1.3.5.4, Repository Investigations; Milestone RI 03-210; January 31, 2003." Carlsbad, NM: Sandia National Laboratories. ERMS 526049. 4.2-1 to 4.2-6.
- Snider, A.C. 2003b. "Verification of the Definition of Generic Weep Brine and the Development of a Recipe for This Brine." Analysis report, April 8, 2003. Carlsbad, NM: Sandia National Laboratories. ERMS 527505.
- Snider, A.C. 2003c. "Calculation of the Quantities of MgO Required for Consumption of CO₂ for the WIPP Compliance Recertification Application." Analysis report, July 3, 2003. Carlsbad, NM: Sandia National Laboratories. ERMS 530220.
- Snider, A.C., and Y.-L. Xiong. 2002. "Carbonation of Magnesium Oxide," "Sandia National Laboratories Technical Baseline Reports; WBS 1.3.5.3, Compliance Monitoring; WBS 1.3.5.4, Repository Investigations; Milestone RI130; July 31, 2002." Carlsbad, NM: Sandia National Laboratories. ERMS 523189. 4.1-1 to 4.1-28.
- Snider, A.C., and Y.-L. Xiong. 2004. "Continuing Investigations of the Hydration and Carbonation of Premier Chemical MgO." Analysis report, October 12, 2004. Carlsbad, NM: Sandia National Laboratories. ERMS 537188.
- Stein, C.L. 1985. *Mineralogy in the Waste Isolation Pilot Plant (WIPP) Facility Stratigraphic Horizon*. SAND85-0321. Albuquerque, NM: Sandia National Laboratories.
- Storz, L.J. 1996. "Estimate of the Amount of Ca(OH)₂ Contained in the Portland Cement Fraction of the Waste for Disposal in the WIPP." Memorandum to Y. Wang., June 24, 1996. Albuquerque, NM: Sandia National Laboratories. ERMS 240351.

- Telander, M.R., and R.E. Westerman. 1993. *Hydrogen Generation by Metal Corrosion in Simulated Waste Isolation Pilot Plant Environments*. SAND92-7347. Albuquerque, NM: Sandia National Laboratories.
- Telander, M.R., and R.E. Westerman. 1997. *Hydrogen Generation by Metal Corrosion in Simulated Waste Isolation Pilot Plant Environments*. SAND96-2538. Albuquerque, NM: Sandia National Laboratories.
- Tracy, R.J., H.W. Jaffe, and P. Robinson. 1978. "Monticellite Marble at Cascade Mountain, Adirondack Mountains, New York," *American Mineralogist*. Vol. 63, 991-999.
- Trovato, E.R. 1997. Untitled letter from E.R. Trovato to G. Dials with enclosures (parameters that are no longer of concern and parameters that DOE must use for the PAVT), April 25, 1997. Washington, DC: U.S. Environmental Protection Agency Office of Radiation and Indoor Air. ERMS 247206.
- Turner, F.J. 1980. *Metamorphic Petrology, Mineralogical, Field and Tectonic Aspects*. New York, NY: Hemisphere Publishing Corporation.
- Twilley, J. 2006. "Raman Spectroscopy Investigations of the Weathering Alteration of a Predazzite Marble Mouflon of the Indus Valley Culture," *Journal of Raman Spectroscopy*. Vol. 37, 1201-1210.
- U.S. DOE. 1996. *Title 40 CFR Part 191 Compliance Certification Application for the Waste Isolation Pilot Plant, Vol. 1-21*. DOE/CAO-1994-2184. Carlsbad, NM: U.S. Department of Energy Carlsbad Area Office.
- U.S. DOE. 2004. *Title 40 CFR Part 191 Compliance Recertification Application for the Waste Isolation Pilot Plant, Vol. 1-8*. DOE/WIPP 2004-3231. Carlsbad, NM: U.S. Department of Energy Carlsbad Field Office.
- U.S. EPA. 1998. "Technical Support Document for Section 194.24: EPA's Evaluation of DOE's Actinide Source Term." EPA Air Docket A-93-02-V-B-17. Washington, DC: U.S. Environmental Protection Agency Office of Radiation and Indoor Air.
- Valley, J.W., and E.J. Essene. 1980. "Calc-Silicate Reactions in Adirondack Marble: The Role of Fluids and Solid Solution," *Geological Society of America Bulletin*. Vol. 91, 114-117.
- Villarreal, R., J.M. Bergquist, and S.L. Leonard. 2001a. *The Actinide Source-Term Waste Test Program (STTP) Final Report, Volume I*. LA-UR-01-6822. Los Alamos, NM: Los Alamos National Laboratory.
- Villarreal, R., J.M. Bergquist, and S.L. Leonard. 2001b. *The Actinide Source-Term Waste Test Program (STTP) Final Report, Volume II*. LA-UR-01-6912. Los Alamos, NM: Los Alamos National Laboratory.
- Villarreal, R., M. King, and S.L. Leonard. 2001c. *The Actinide Source-Term Waste Test Program (STTP) Final Report, Volume IV*. LA-UR-01-6914. Los Alamos, NM: Los Alamos National Laboratory.

- Villarreal, R., A.C. Morzinski, J.M. Bergquist, and S.L. Leonard. 2001d. *The Actinide Source-Term Waste Test Program (STTP) Final Report, Volume III*. LA-UR-01-6913. Los Alamos, NM: Los Alamos National Laboratory.
- Wall, N.A. 2005. "Preliminary Results for the Evaluation of Potential New MgO." Carlsbad, NM: Sandia National Laboratories. ERMS 538514.
- Wall, N.A., and D. Enos. 2006. "Iron and Lead Corrosion in WIPP-Relevant Conditions, TP 06-02, Rev. 1." April 24, 2006. Carlsbad, NM: Sandia National Laboratories. ERMS 543238.
- Wang, Y. 1998. "WIPP PA Validation Document for FMT (Version 2.4), Document Version 2.4." Carlsbad, NM: Sandia National Laboratories. ERMS 251587.
- Wang, Y. and L.H. Brush. 1996. "Estimates of Gas-Generation Parameters for the Long-Term WIPP Performance Assessment." Memorandum to M.S. Tierney, January 26, 1996. Albuquerque, NM: Sandia National Laboratories. ERMS 231943.
- Wells, L.S., and K. Taylor. 1937. "Hydration of Magnesia in Dolomitic Hydrated Limes and Putties," *Journal of Research of the National Bureau of Standards*. Vol. 19, 215-236.
- Wolery, T.J. 1992a. *EQ3/6, A Software Package for Geochemical Modeling of Aqueous Systems: Package Overview and Installation Guide (Version 7.0)*. UCRL-MA-110662 PT I. Livermore, CA: Lawrence Livermore National Laboratory.
- Wolery, T.J. 1992b. *EQ3NR, A Computer Program for Geochemical Aqueous Speciation-Solubility Calculations: Theoretical Manual, User's Guide, and Related Documentation (Version 7.0)*. UCRL-MA-110662 PT III. Livermore, CA: Lawrence Livermore National Laboratory.
- Wolery, T.J., and S.A. Daveler. 1992. *EQ6, A Computer Program for Reaction-Path Modeling of Aqueous Geochemical Systems: Theoretical Manual, User's Guide, and Related Documentation (Version 7.0)*. UCRL-MA-110662 PT IV. Livermore, CA: Lawrence Livermore National Laboratory.
- WTS. 2005. "Specification for Prepackaged MgO Backfill." Specification D-0101, Rev. 5. May 12, 2005. Carlsbad, NM: Westinghouse Electric Corp. TRU Solutions.
- Xiong, Y.-L., and A.C. Snider. 2003. "Carbonation Rates of the Magnesium Oxide Hydration Product Brucite in Various Solutions," "Sandia National Laboratories Technical Baseline Reports; WBS 1.3.5.3, Compliance Monitoring; WBS 1.3.5.4, Repository Investigations; Milestone RI 03-210; January 31, 2003." Carlsbad, NM: Sandia National Laboratories. ERMS 526049. 4.3-1 to 4.3-11.
- Zhang, P.-C., H.L. Anderson, J.W. Kelly, J.L. Krumhansl, and H.W. Papenguth. 2000. "Kinetics and Mechanisms of Formation of Magnesite from Hydromagnesite in Brine," submitted to *Applied Geochemistry*. Albuquerque, NM: Sandia National Laboratories. ERMS 514868.

9 TABLES

Table 1. Effects of Temperature Used for LOI Analysis of MgO Hydration Products on the Brucite + Portlandite Contents^A of the Samples (from Wall, 2005, Table 1, unless otherwise noted).

Material	Temperature Used for LOI			
	500 °C		750 °C	
	Mole %	Wt %	Mole %	Wt %
WTS-20	87 ± 5 ^B	91 ± 4 ^B	ND ^C	ND ^C
WTS-30	87 ± 5 ^B	91 ± 4 ^B	96 ± 5 ^B	97 ± 3 ^B
WTS-60	90 ± 3 ^B	93 ± 2 ^B	ND ^C	ND ^C
Premier	84.6 ^D	88.8 ^D	89 ^D	92 ^D

- A. Snider and Xiong (2004) and Wall (2005) reported their results of LOI analysis of MgO hydration products as mole % brucite or wt % brucite. However, Deng et al (2006) report their results as mole % brucite + portlandite or wt % brucite + portlandite. We report all these results as mole % brucite + portlandite or wt % brucite + portlandite.
- B. Reported uncertainties represent two standard deviations (2σ).
- C. ND = not determined.
- D. Snider and Xiong (2004).

Table 2. Results of Chemical Analysis and LOI Testing of WTS-60 (Deng et al., 2006b).

Material	Mol %	Wt %
WTS-60	96 ± 2	96 ± 2

Table 3. Results of Field Studies of Contact-Metamorphosed Dolomite and Mg-bearing Limestone.

Locality	Periclase Present	Brucite After Periclase	Reference(s)
Adamello (Italy)	No	Yes	Gerdes et al. (1999)
Adirondacks (New York)	No	Yes	Tracy et al. (1978), Valley and Essene (1980)
Alta (Utah)	?, A	Yes	Moore and Kerrick (1976)
Ballachulish (Scotland)	?, B	Yes	Masch and Heuss-Abbichler (1991), Ferry (1996)
Beinn an Dubhaich (Scotland)	No	Yes	Ferry and Rumble (1997)
Crestmore (California)	No	Yes	Burnham (1959) Carpenter (1967)
Elkhorn (Montana)	No	Yes	Bowman and Essene (1982, 1984)
Granåsen (Sweden)	No	Yes	Øvereng (2000)
Monzoni (Italy)	No	Yes	Ferry et al. (2002)
Predazzo (Italy)	No	Yes	Ferry et al. (2002)
Sierra Nevada (California)	No	Yes	Kerrick et al. (1973), Ferry (1989)
Silver Star (Montana)	No	Yes	Ferry and Rumble (1997)
Ubehebe Peak (California)	No	Yes	Roselle (1997), Roselle et al. (1999), Kozak et al. (2004)

- A. The reported periclase may in fact be clinohumite, which is not easily distinguishable from periclase.
 B. Masch and Heuss-Abbichler (1991) report periclase, but Ferry (1996) claims all periclase replaced by brucite.

Distribution:

MS 0776 E.J. Nowak (Org. 6852)
MS 1395 M.J. Chavez (Org. 6820)
MS 1395 J.R. Trone (Org. 6820)
MS 1395 G.R. Kirkes (Org. 6821)
MS 1395 C.D. Leigh (Org. 6821)
MS 1395 J.W. Garner (Org. 6821)
MS 1395 J.F. Kanney (Org. 6821)
MS 1395 M.B. Nemer (Org. 6821)
MS 1395 E.D. Vugrin (Org. 6821)
MS 1395 S.W. Wagner (Org. 6821)
MS 1395 M.J. Rigali (Org. 6822)
MS 1395 H. Deng (Org. 6822)
MS 1395 C.G. Herrick (Org. 6822)
MS 1395 S.R. Johnsen (Org. 6820)
MS 1395 Y.-L. Xiong (Org. 6822)
MS 1395 L.H. Brush (Org. 6822)
MS 1395 S.L. Casey (Org. 6822), for submittal to the SNL/WIPP Records Center (2 copies)